CONTENTS

Geofysiske Publikasjoner, Vol. XVI, No. 12.
Utgitt av Det Norske Videnskaps-Akademi i Oslo.

THE MEAN FIELD OF DISTURBANCE OF THE POLAR EARTH-MAGNETIC STORM

BY
LEIV HARANG

(Manuscript received Sept. 20th, 1945.)

Section I.

I. INTRODUCTION

In his classical work, The Norwegian Aurora Polaris Expedition 1902—03[1], Birkeland has given results of his comprehensive studies of the field of disturbance of earth-magnetic storms, in which the characteristics of the main types of disturbances were discovered. Birkeland studied the position and changes of the perturbing vector (principally the perturbing vector in the horizontal plane, P_H, and the perturbing vector in vertical direction) during the progress of the storms, and, by drawing up these on maps at certain time intervals, the types of perturbations could be identified in principally the same way as the properties of the air masses in meteorology on the synoptic charts later introduced.

The chief results of his studies of the disturbance fields were the discoveries of the positive and negative polar elementary storms and the equatorial storms, also of the positive and negative type. For observatories lying near the auroral zone the effects of the polar storms are by far the strongest, and in averaging the storm effects at a polar station the effects of the equatorial storms are of little importance. The effects of the polar disturbances on the other hand diminish very rapidly with decreasing latitudes, and for stations near the equator the equatorial disturbances, and especially that of the positive type, are the most important.

Birkeland's point of view for studying the earth-magnetic storms requires a dense net of recording stations, and especially at the storm centres near the auroral zone the net must be by far denser than the number of permanent recording stations.

During the Polar-Year 1932—33 a number of recording stations were in action especially north and south of the auroral zone from Scandinavia over Bear Island to Spitzbergen and Greenland. This set of recording stations therefore made it possible to study in detail more precisely than ever before the character of disturbance along the auroral zone north of Scandinavia. The material has already been used to some extent by Vestine[1], Vestine and Chapman[2] and McNish[3] in their studies of the dimensions and positions of the assumed electrical current systems producing the elementary polar storm.

When averaging the storm effects at a polar station, one will always have to do almost only with the effect of the elementary polar storm. Vestine in his study, used the mean annual disturbance vector at a number of stations and demonstrated very strikingly the change in direction and magnitude of the perturbing vector when crossing the auroral zone along a meridian from north to south. Assuming, as Birkeland did, the elementary polar storm to be caused by a narrow electrical current flowing along the auroral zone, the mean position of the current — and the assu-

[1] Vol. I, Section 1 and 2, 1—801 pages, Christiania (Oslo) 1908 and 1913.

[1] Vestine, Terr. Mag. *43*, 261 (1938).
[2] Vestine and Chapman, Terr. Mag. *43*, 351 (1938).
[3] McNish, Terr. Mag. *43*, 67 (1938).

med identical position of the auroral zone — was determined with an accuracy of less than a degree in latitude.

2. THE MODE OF REPRESENTATION OF THE FIELD OF DISTURBANCE

Birkeland demonstrated the field of disturbance, which we now in accordance with the usual designation will call the D-field, by plotting the vectors of disturbance at different observatories at certain time intervals on maps. A series of such maps thus gave an excellent illustration of the dynamical character of the different individual storms. The scope of the present investigation is, however, to study the *mean* position of the D-fields for various degrees of storminess. Further, to study the diurnal variation and displacement of the same mean fields in order to explain certain characteristics of the mean annual vector diagrams of storminess recorded in Tromsø.

The starting point has been the fact already pointed out by Birkeland[1] that the average polar storm at stations near the auroral zone exhibits a diurnal variation which only depends on local time. This was evident, according to Birkeland, for polar stations lying over a range of latitudes from Iceland over Northern Norway and Spitzbergen to Novaya Zembla. The maximum of the positive disturbance (*i.e.* the maximum of positive deflection in horizontal intensity) appeared in mean at 16.8^h and the maximum of negative disturbance (*i.e.* the maximum of negative deflection in the horizontal intensity) appeared in mean at 24.5^h local time. We may therefore roughly assume that the mean D-field, for the range of longitudes here in question, was moving from west to east with the rotation of the earth.

A number of recording stations was therefore selected lying within a small range of longitudes, but covering a range of latitudes from about $\Phi = 55°$ to $75°$ (Φ being the geomagnetic latitude), thus crossing the auroral zone in N—S direction approximately at ninety degrees. This belt of stations should thus record the changes of the mean D-field when this was moving uniformly from west to east in the course of the day. The observatories used are listed in Table 1.

Table 1.

	φ	λ	Φ	Λ
Angmagssalik	65.6	322.4	74.2	52.7
Sveagruvan	77.9	16.8	73.9	130.7
Bear Island	74.5	19.2	71.1	124.5
Tromsø	69.7	18.9	67.1	116.7
Bossekop	70.0	23.2	66.6	120.4
Petsamo	69.5	31.2	64.9	125.8
Sodankylä	67.4	26.6	63.8	120.0
Lerwick	60.1	358.8	62.5	88.6
Lovø	59.4	17.8	58.1	105.8
Rude Skov	55.8	12.4	55.8	98.5
de Bilt	52.1	5.2	53.8	89.6

Here are (φ, λ) the geographical coordinates and (Φ, Λ) the geomagnetic coordinates reckoned from the magnetic axis' point and the zero meridian through the axis' point and geographical North Pole. Fig. 1 shows the distribution of the observatories in geomagnetic coordinates.

The distribution of the observatories are especially favourable just south of the auroral

[1] loc. cit. p. 538.

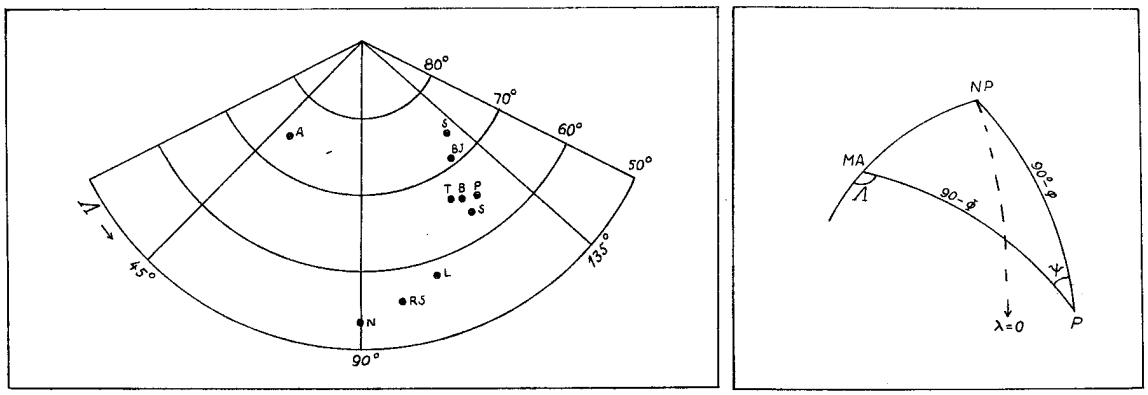

Fig. 1 and 2. Distribution of observatories used. (Φ, Λ) are the geomagnetic coordinates, NP is geographical north-pole and MA is earth-magnetic axis' point.

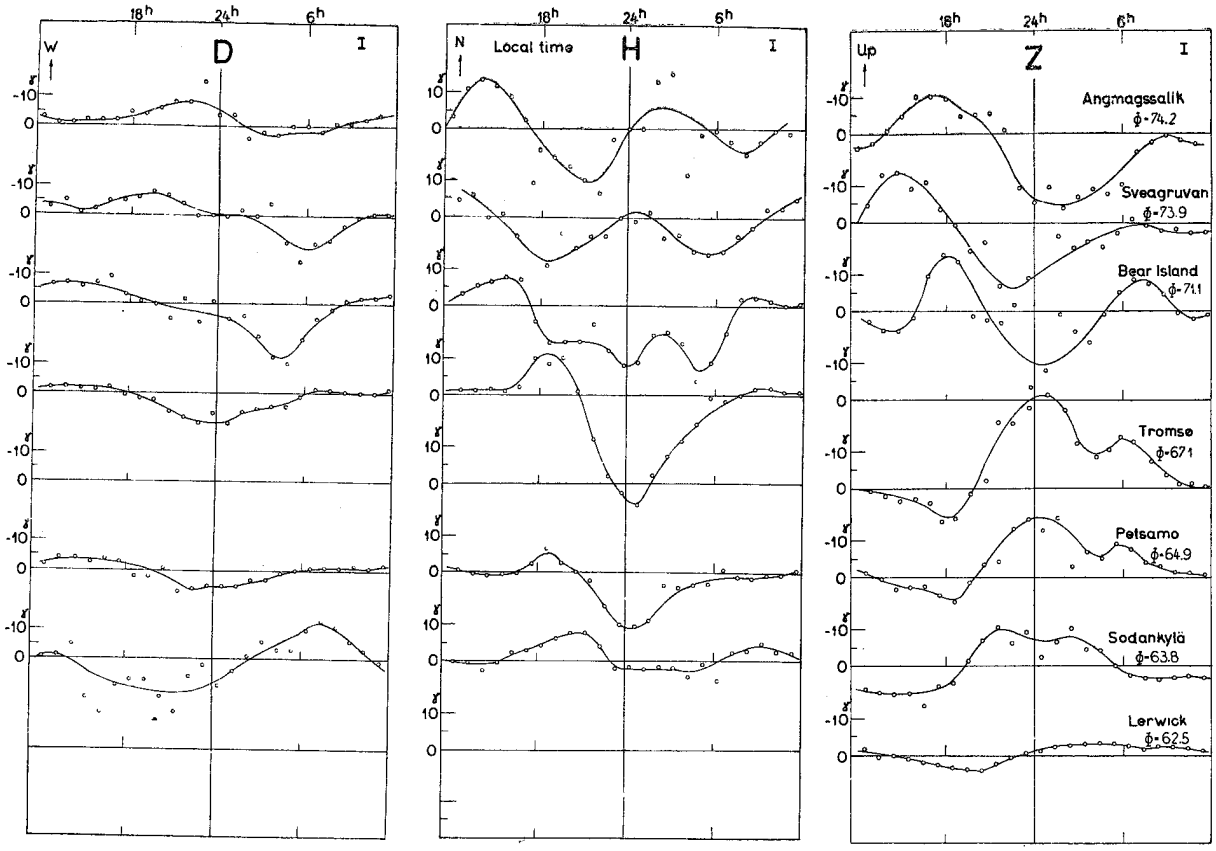
18h
24h
6h
W
D
I
N
Local time
H
Up
Z
Angmagssalik
φ=74.2
Sveagruvan
φ=73.9
Bear Island
φ=71.1
Tromsø
φ=67.1
Petsamo
φ=64.9
Sodankylä
φ=63.8
Lerwick
φ=62.5

Fig. 3 a.

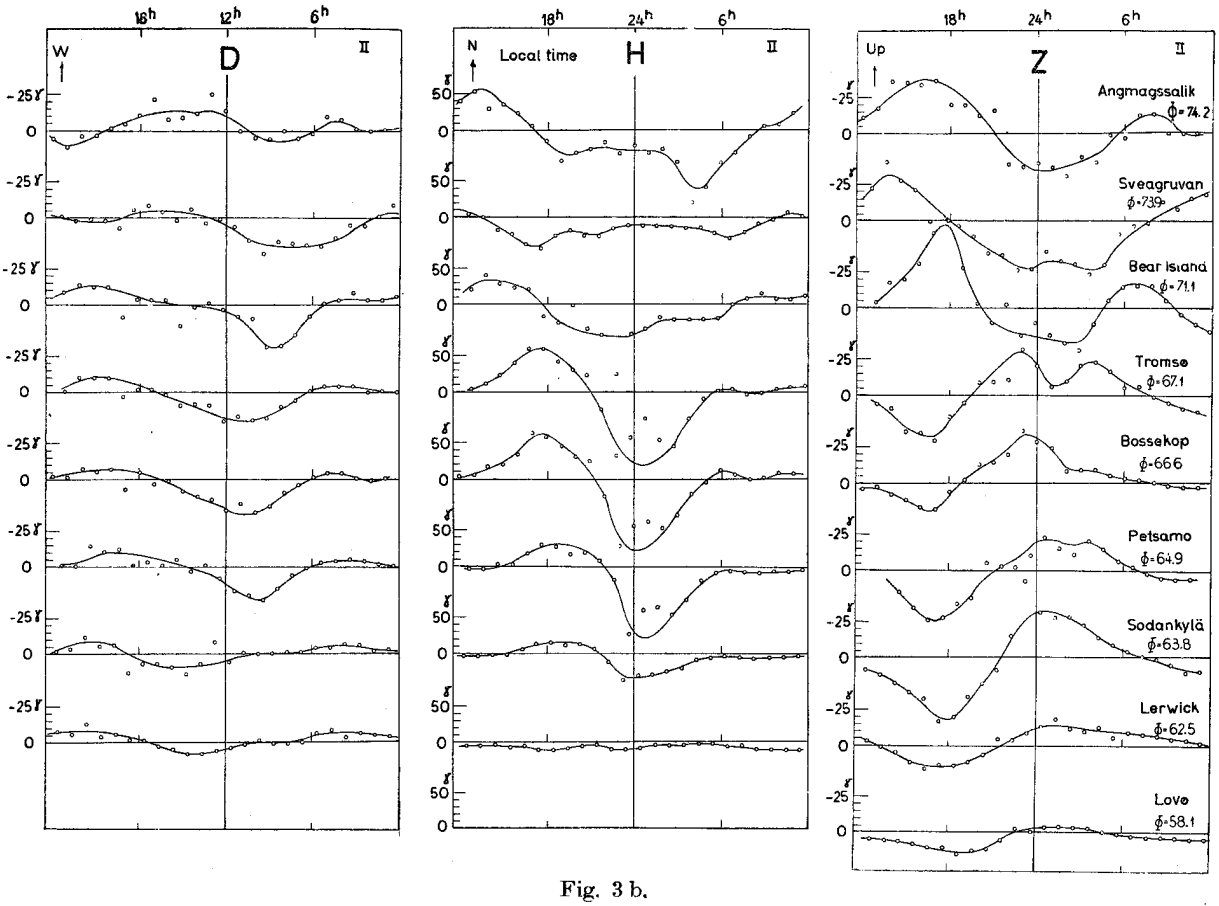
18h
12h
6h
W
D
II
N
Local time
H
Up
Z
Angmagssalik
φ=74.2
Sveagruvan
φ=73.9
Bear Island
φ=71.1
Tromsø
φ=67.1
Bossekop
φ=66.6
Petsamo
φ=64.9
Sodankylä
φ=63.8
Lerwick
φ=62.5
Lovo
φ=58.1

Fig. 3 b.

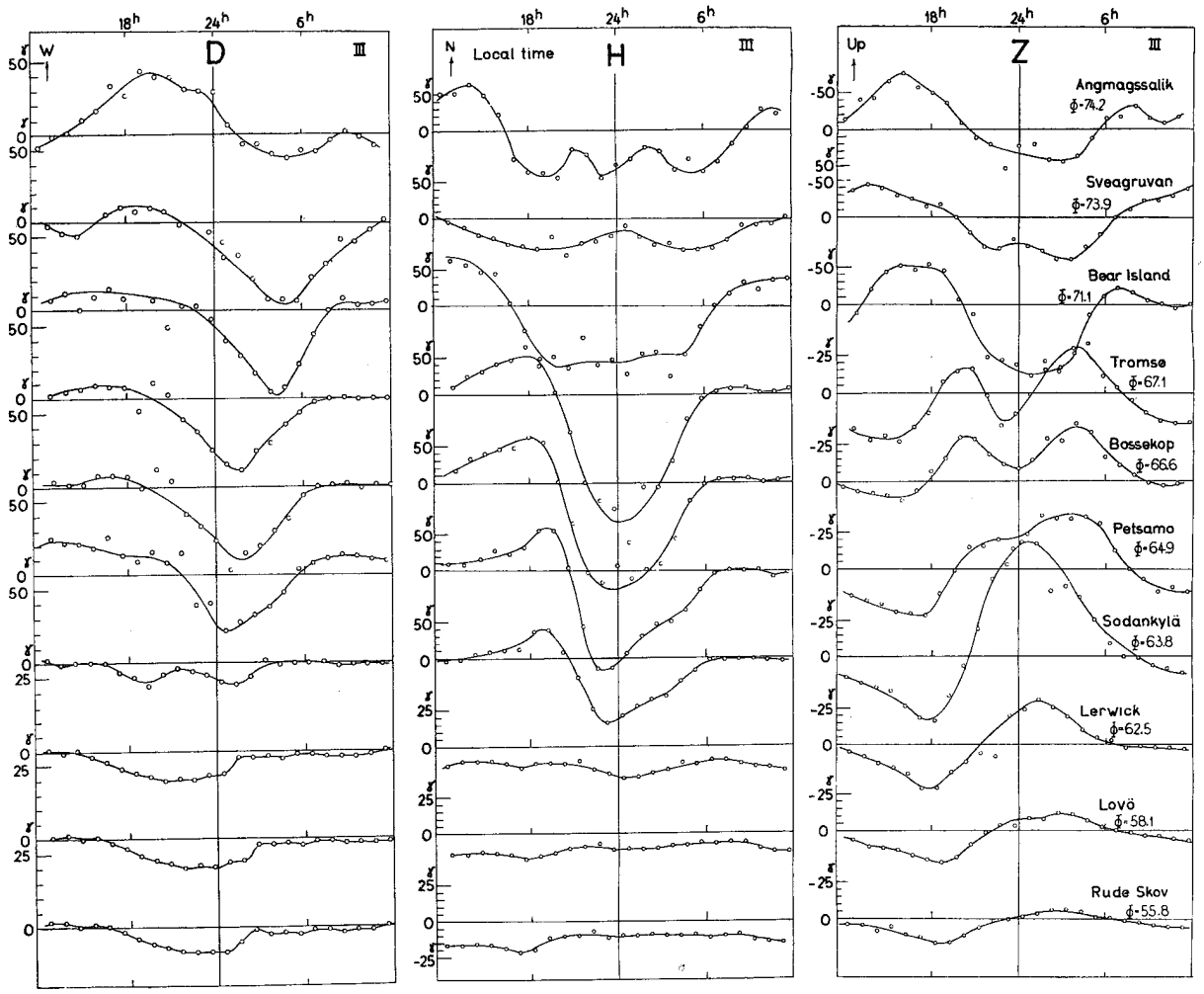

Fig. 3 c.

zone at about $\Phi = 67°$. North of the zone there are the two valuable stations at Bear Island and Sveagruvan, whereas Angmagssalik lies somewhat outside the range of longitudes of the rest of the observatories.

From auroral observations it is well known that the strong aurorae appearing at lower latitudes are always accompanied by strong earth-magnetic disturbances. Quantitatively this effect has been studied by Røstad[1], who compared the position of the aurorae with the magnitude of disturbance recorded at Potsdam. In this connection it would be of special interest to study the position of the mean D-fields for various degrees of storminess.

Now Tromsø is the station which lies most closely to the auroral zone and, accordingly, should be the place where the degree of storminess in H was the most direct measure for the current density of the disturbing currents. During the Polar Year 1932—33 the days where therefore classified into four groups, I, II, III and IV, according to the values of the daily sums of the storminess in the horizontal intensity recorded in Tromsø.

Table 2.

Class	Corresponding to a daily sum of storminess (ΣS) in H lying in range of	Number of days used	Mean values of international character figure, C
I	0— 500 gammas	19	0.32
II	500—1000 »	10	0.75
III	1000—2000 »	15	1.07
IV	> 2000 »	20	1.43

For Tromsø the hourly values of storminess are tabulated in the year books. For the other observatories the hourly stormines values had to

[1] Geofys. Publ. *5*, No. 5 (Oslo).

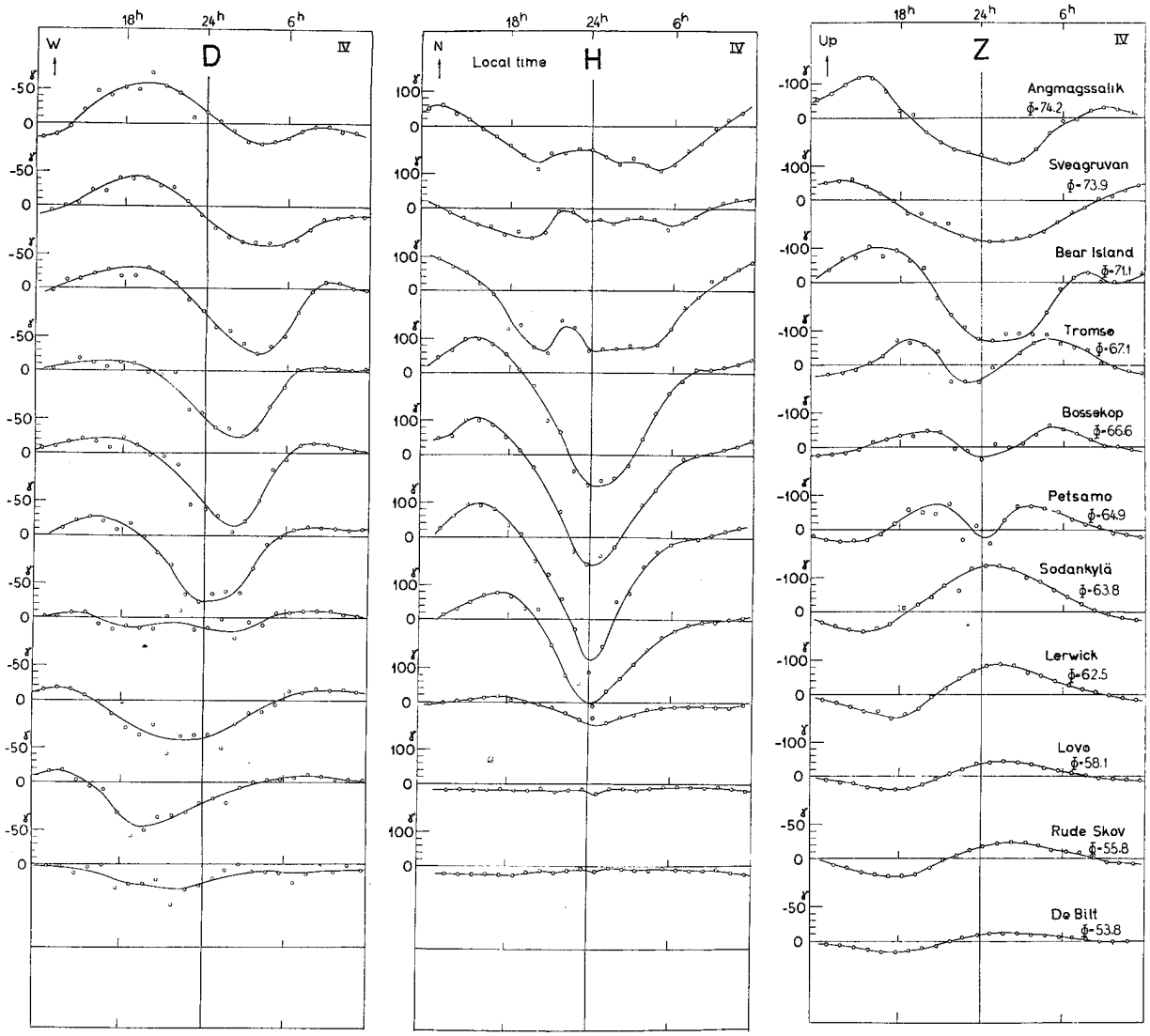

Fig. 3 d.

Fig. 3 a, b, c and d. Diurnal variation of S_D in gammas in the four ranges of disturbance I, II, III and IV at the observatories considered and arranged according to local time.

be computed for each of the days selected. This was done by subtracting the hourly values on quiet days which appeared just before and after the disturbed day considered.

Usually, the hourly values in the year books are tabulated in the succession 0^h to 24^h. The polar storms, however, show a pronounced maximum at midnight, and for characterizing the earth-magnetic activity the range 0^h—24^h is physically unsuitable. A polar perturbation usually starts with a positive perturbation at 14^h—16^h, reaches its maximum at midnight with a strong negative decrease in H, and dies out in the course of the morning hours. The period from 12^h to 12^h usually comprises the time of action of a normal polar storm, and the hourly values used at all the observatories selected were re-arranged according to this time-interval. For each of the observatories used the storminess was arrenged according to *local* time. The *mean* hourly values for each of the four classes of disturbance thus give the mean solar diurnal variation of disturbance, in the literature now usually designated with S_D, for each of the three components.

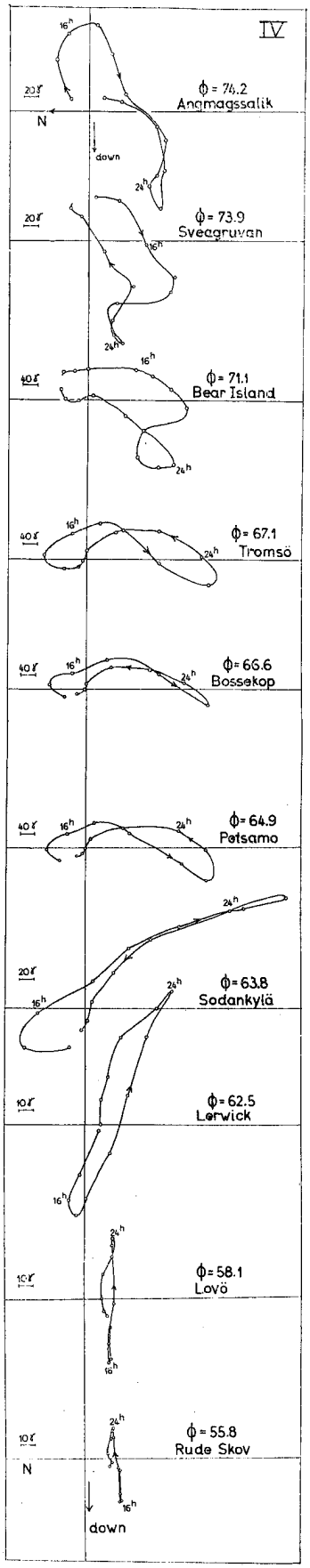

Fig. 4. Diurnal variation of the storminess (S_D) in a vertical plane lying in N—S direction. Range IV.

In Table 3 are given the mean values of S_D at the observatories considered, separated in four ranges according to the magnitudes of disturbance.

In fig. 3 are shown the diurnal variations of S_D.

For range I and partly also for II, fig. 3 shows that there is a considerable scattering of the individual values from the mean curve. In these cases the values of storminess are small, and a greater number of days should be used in order to get smooth curves. For class IV, where the values of storminess are great and easy to determine with accuracy, we get smooth mean curves gradually being transformed along the whole range of observatories with decreasing values of Φ. A common feature for all ranges is that the mean curves for the three observatories Bear Island, Sveagruvan and Angmagssalik, all lying *north* of the auroral zone, are much more irregular than the curves obtained at observatories lying south of the auroral zone. We regard this as real, and we get the impression that the currents producing the earth-magnetic disturbances are on the southern edge of the auroral zone moving regularly and spreading uniformly southwards, whereas on the northern, or inner, edge of the auroral zone, the currents are moving far more irregularly often forming systems of whirls.

The curves for S_D in D show a regular and gradual change from the one observatory to the other in the whole range of Φ. In H there is a maximum of amplitudes at the latitude of about Tromsø. In Z the deflections are reversed for observatories lying north and south of the auroral zone. There is, however, an interesting feature for observatories lying just below the auroral zone. Here the curve in Z appears as a double wave. This double wave appears in all four ranges and is undoubtedly real. As we shall see later, this is explained by a discontinuity appearing in the current system (or auroral zone).

In fig. 3 the diurnal variation of the three components of the storminess are presented separately. Another mode of representation of the diurnal variation often used, is a diagram representing the combined variation of the storminess in H and Z in a vertical plane lying in N—S direction. In fig. 4 the diurnal variation of the H, Z-vector is shown for range IV. Each point marked out on the curve is the end of a vector from origo to the point at each hour of the day. The vector diagrams show a gradual transformation from northern to southern latitudes. We see that for stations lying just below the auroral zone — Tromsø, Bossekop and Petsamo — the changes in the vector are greatest in N—S direction. With increasing distances from the auroral zone the relative changes increase in the Z-direction.

The next step would be to get an impression of the gradual change of the D-field over Scandinavia in the course of the day. From fig. 3 it is evident that the diurnal variation of S_D in H and Z solely depends on local time for the region here considered. In D there is a gradual change with increasing values of Φ. In order to get more complete dates for demonstration of the D-field, the mean values for each degree and hour (Φ, t) was determined by an interpolation process. From table 3 the hourly values were drawn up graphically as a function of Φ. Fig. 5

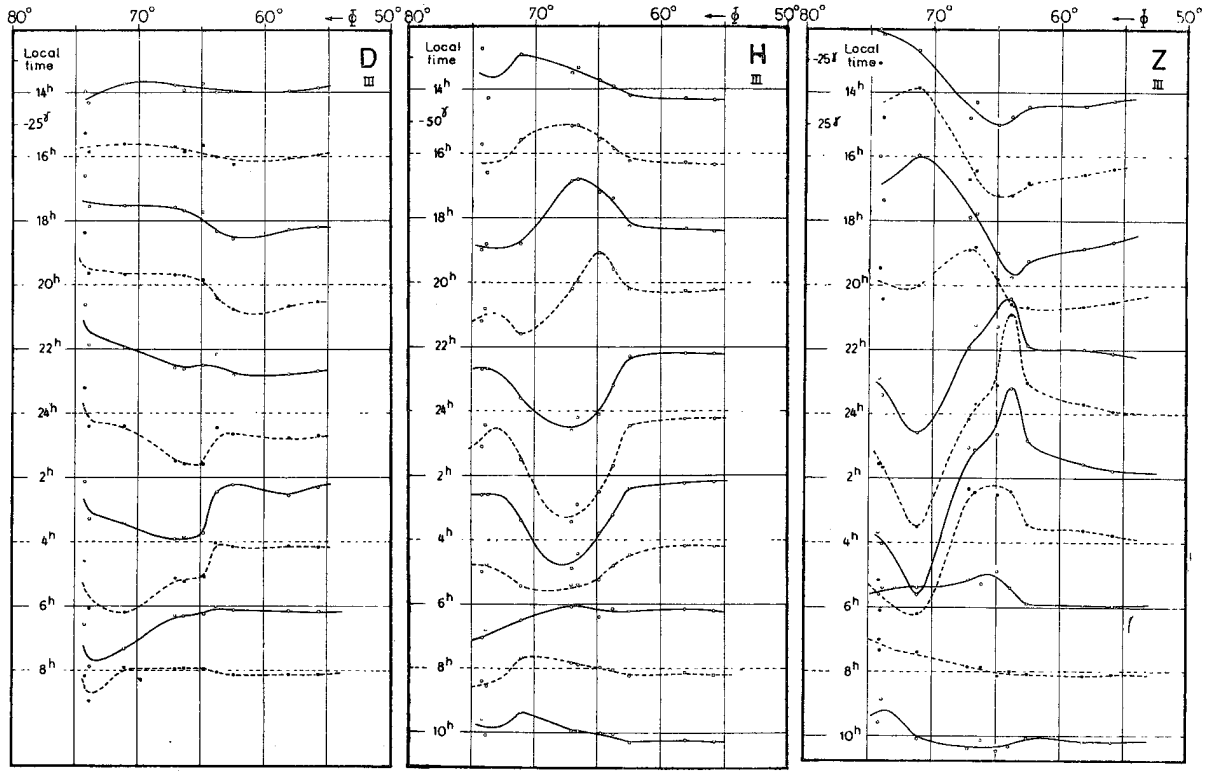

Fig. 5. Variation of the mean hourly values of storminess (S_D) with latitudes, Φ, at different hours of the day, local time. The curves given are only for range III and only for each two hours.

shows a number of such curves for range III. The curves drawn up thus represent the mean smoothed values of the variation of the hourly values of S_D along a geomagnetic meridian at the hour chosen. These mean curves are of considerable interest. We see how the values of the storminess in H show a distinct maximum at 16^h and 24^h, cooresponding to maximum positive and negative disturbance, and in Z we have a wave-formed curve which is zero for the value of Φ at which H has its maximum. We thus have a graphical determination of the latitude of the current system producing the positive and negative disturbances. This is principally the same as in Vestine's[1] analysis of the dates previously quoted, but as we shall see later the whole disturbance field comes out in more detail in the further analysis.

In Table 4 are given the results of this graphical determination of the values of storminess for each set of (Φ, t)-values.

In order to get a complete picture of the changes of the disturbance vector in the course of the day *across the belt of observatories* used in this analysis, we give a graphical representation of the values in table 4 for each of the components of the disturbance vector.

A projection of map was calculated in which the cone touched the earth at the 65° latitude circle and folded out, this projection giving a fairly correct representation of the areas in the region of the auroral zone. The circles of latitudes represent *geomagnetic* latitudes and the lines of longitudes represent local time. For each set of values of (Φ, t), the corresponding values of the components of the disturbance vector were plotted down on a set of three maps, and the lines of equal values of S_D (or respectively $\triangle$D, $\triangle H$ and $\triangle Z$ as used on the maps) were drawn up by interpolation. For each of the four ranges we thus have a set of three maps giving a graphical representation in isopletes of the variation of the three components of a vector, each set thus giving the variation of the D-field for the four ranges of intensities. In order to avoid any misunderstanding we would again point out that these maps represent the variation of the D-field with local time in the course of a day over Scandinavia,

[1] Vestine, Terr. Mag. *43*, 261 (1938).

Table 3. Mean diurnal variation of Storminess (S_D)
Polar Year

	Station	Local 12	13	14	15	16	17	18	19	20	21	22	23	24
	Range I.													
Declination.	Angmagssalik	2.5	1.5	1.0	1.5	1.5	2.0	3.5	5.0	6.0	7.5	8.0	7.5	6.5
	Sveagruvan	2.0	2.0	2.5	2.0	3.0	4.5	6.0	7.0	7.0	5.0	2.5	1.5	0
	Bear Island	4.0	5.0	6.5	6.5	6.0	5.0	3.5	1.5	— 1.0	— 2.0	— 2.5	— 3.0	— 3.0
	Tromsø	2.0	2.0	2.0	2.0	2.0	1.5	0.5	— 1.0	— 3.5	— 6.5	— 8.5	— 10.0	— 10.5
	Petsamo	2.0	2.0	3.0	3.0	3.5	3.0	2.0	0	— 2.5	— 5.0	— 6.5	— 6.0	— 5.5
	Sodankylä	0	1.0	0	— 4.0	— 7.0	— 8.0	— 8.0	— 9.0	— 10.0	— 10.0	— 10.0	— 9.0	— 8.0
Hor. Intensity.	Angmagssalik	11.0	16.0	18.0	19.0	14.0	8.0	2.0	— 2.5	— 6.0	— 8.0	— 7.0	— 1.0	5.5
	Sveagruvan	4.6	4.8	5.0	2.0	— 1.5	— 5.5	— 10.0	— 11.6	— 10.6	— 8.0	— 5.5	— 3.0	0
	Bear Island	11.0	14.2	15.0	8.0	— 8.0	— 18.0	— 19.7	— 21.0	— 24.0	— 28.0	— 29.0	— 26.0	— 20.2
	Tromsø	1.2	1.2	1.3	2.0	4.3	8.5	10.0	9.0	— 2.0	— 14.0	— 21.0	— 29.0	— 29.0
	Petsamo	1.2	0	— 0.5	— 1.1	— 0.6	1.1	4.0	4.5	3.0	— 1.0	— 5.0	— 11.0	— 15.0
	Sodankylä	0.5	— 0.2	— 0.3	— 0.3	0.3	1.0	2.0	2.7	3.5	3.6	2.7	0.5	— 1.0
Ver. Intensity.	Angmagssalik	2.5	2.0	0	— 4.0	— 8.0	— 10.0	— 11.0	— 9.5	— 6.0	— 1.0	6.5	13.0	18.0
	Sveagruvan	— 4.0	— 11.0	— 13.0	— 12.5	— 11.0	— 7.0	— 2.5	2.0	6.5	11.5	15.0	16.0	15.0
	Bear Island	2.5	4.0	5.5	4.0	— 2.0	— 11.0	— 13.0	— 12.5	— 6.0	1.0	4.5	8.5	11.0
	Tromsø	0.5	1.5	4.5	6.5	7.0	6.5	4.0	0	— 6.0	— 13.0	— 18.5	— 22.5	— 23.0
	Petsamo	— 1.0	0	1.5	3.0	3.5	4.5	5.0	3.0	0	— 4.0	— 9.0	— 13.0	— 15.0
	Sodankylä	— 2.0	1.0	0	1.0	2.0	2.5	2.5	1.5	— 2.0	— 6.0	— 10.0	— 13.0	— 14.0
	Lerwick	— 0.7	0	0.3	1.0	1.7	2.3	3.0	3.5	4.0	3.5	1.7	— 0.3	— 1.5
	Range II.													
Declination.	Angmagssalik	— 6	— 10	— 8	— 4	2	6	10	13	14	14	14	14	13
	Sveagruvan	3	0	— 3	— 4	3	— 1	3	5	5	4	2	— 1	— 4
	Bear Island	7	10	12	11	8	6	5	1	0	— 1	— 2	— 3	— 4
	Tromsø	0	5	10	9	8	5	3	1	— 3	— 7	— 10	— 14	— 18
	Bossekop	2	2	4	6	7	7	5	2	— 2	— 7	— 12	— 16	— 20
	Petsamo	1	0	5	10	10	9	7	6	3	2	— 2	— 5	— 12
	Sodankylä	2	2	5	8	6	2	— 5	— 8	— 9	— 10	— 9	— 8	— 5
	Lerwick	4	5	6	6	6	3	2	— 3	— 5	— 7	— 9	— 8	— 6
Hor. Intensity.	Angmagssalik	41	52	50	35	20	5	— 15	— 27	— 29	— 26	— 22	— 22	— 22
	Sveagruvan	3	1	— 9	— 20	— 32	— 38	— 37	— 27	— 22	— 24	— 22	— 15	— 12
	Bear Island	14	23	33	27	20	5	— 12	— 26	— 35	— 41	— 44	— 46	— 43
	Tromsø	6	10	15	26	43	58	53	42	30	10	— 30	— 60	— 84
	Bossekop	5	10	14	23	36	55	58	49	32	10	— 24	— 55	— 88
	Petsamo	— 6	— 3	0	3	7	18	25	28	23	16	0	— 40	— 82
	Sodankylä	— 4	— 4	— 2	— 1	3	11	16	17	15	10	— 5	— 25	— 36
	Lerwick	— 8	— 6	— 6	— 7	— 8	— 10	— 12	— 11	— 8	— 6	— 8	— 11	— 10
Ver. Intensity.	Angmagssalik	— 10	— 19	— 27	— 34	— 37	— 35	— 30	— 23	— 13	0	10	20	25
	Sveagruvan	— 19	— 22	— 30	— 24	— 15	— 6	2	8	14	20	27	30	30
	Bear Island	15	1	— 15	— 24	— 35	— 51	— 44	— 30	— 15	— 1	10	17	20
	Tromsø	10	12	15	22	26	25	14	3	— 5	— 14	— 23	— 27	— 20
	Bossekop	2	3	8	13	16	17	9	— 2	— 9	— 16	— 26	— 35	— 32
	Petsamo	13	14	17	20	30	34	31	23	15	5	— 4	— 11	— 17
	Sodankylä	9	10	17	24	32	37	38	32	22	12	— 6	— 20	— 28
	Lerwick	— 1	— 1	3	8	12	15	16	12	8	2	— 3	— 8	— 13
	Lovø	5	6	7	8	10	12	16	19	19	10	5	1	— 2

in gammas at different observatories.

1932—33.

time

1	2	3	4	5	6	7	8	9	10	11	*PS*	*NS*	*AS*	*PS—NS*
3.0	0	— 2.0	— 2.5	— 1.5	— 1.5	— 1.5	0	2.0	3.5	3.0	66	9	75	57
0	0	— 2.0	— 7.0	— 11.0	— 11.0	— 10.0	— 6.0	— 2.0	0	1.5	47	49	96	— 2
— 5.0	— 8.0	— 15.0	— 18.0	— 17.0	— 10.0	— 4.0	0	1.5	2.0	2.5	44	88	132	— 44
— 9.0	— 6.5	— 5.0	— 4.0	— 3.5	0	1.5	1.5	0.5	0.5	1.5	17	68	85	— 51
— 5.0	— 4.5	— 3.5	— 2.5	— 1.0	0	1.0	1.0	1.5	1.5	1.5	24	42	66	— 18
— 5.0	— 2.0	2.0	3.0	5.0	8.0	11.0	10.0	7.3	3.0	— 1.0	50	91	141	— 41
12.0	17.5	20.0	17.5	10.0	3.0	— 0.5	— 1.0	2.0	4.0	6.0	185	26	211	159
1.2	— 1.0	— 4.5	— 8.0	— 10.0	— 10.4	— 8.0	— 4.2	— 1.0	— 2.0	3.7	23	103	126	— 80
— 20.4	— 28.0	— 32.5	— 28.0	— 12.0	0	3.5	2.2	1.0	2.2	7.0	64	315	389	— 251
— 22.0	— 16.0	— 11.0	— 7.0	— 4.0	— 1.5	1.0	2.0	2.0	1.0	1.0	44	156	200	— 112
— 15.5	— 12.0	— 8.5	— 6.5	— 3.8	— 2.2	— 1.6	— 1.2	— 1.0	— 0.8	0.2	14	87	101	— 73
— 1.3	— 1.5	— 1.5	— 1.5	— 1.5	— 0.9	0.3	1.2	1.6	1.5	1.0	22	10	32	12
20.0	20.0	18.5	16.0	12.5	9.0	5.0	2.5	1.5	2.0	3.0	152	50	202	102
12.5	10.0	8.0	5.5	3.5	1.5	0	0.5	1.0	2.0	0.5	111	61	172	50
12.0	11.0	8.5	4.0	— 1.0	— 5.5	— 8.0	— 8.0	— 5.5	— 2.0	0.5	77	75	152	2
— 21.0	— 16.0	— 10.0	— 10.0	— 11.5	— 10.5	— 7.0	— 3.0	— 1.0	— 0.5	0	31	173	204	— 142
— 16.0	— 15.0	— 12.0	— 8.0	— 6.5	— 7.5	— 7.5	— 5.0	— 3.0	— 2.0	— 1.5	20	126	146	— 106
— 14.0	— 14.0	— 13.0	— 12.0	— 10.5	— 8.5	— 6.4	— 4.5	— 3.0	— 3.0	— 2.5	10	138	149	— 128
— 2.3	— 3.0	— 3.2	— 3.3	— 3.3	— 3.2	— 3.0	— 2.5	— 2.0	— 2.0	— 1.5	21	32	53	— 11
4	— 4	— 6	— 5	— 4	0	6	7	2	0	— 3	119	50	169	69
— 12	— 17	— 19	— 18	— 18	— 18	— 17	— 13	— 8	— 3	3	25	159	184	— 134
— 8	— 20	— 28	— 27	— 18	— 7	2	3	4	4	5	78	118	196	— 40
— 19	— 20	— 16	— 10	— 4	2	5	5	3	2	1	59	121	180	— 62
— 23	— 23	— 19	— 10	— 4	2	4	4	2	0	1	48	136	184	— 88
— 18	— 23	— 21	— 12	— 4	1	3	3	4	3	2	69	97	166	— 28
— 2	— 1	0	1	1	3	4	5	6	3	2	50	57	107	— 7
— 4	— 1	0	— 1	0	3	5	5	5	5	4	59	44	103	15
— 25	— 34	— 50	— 65	— 63	— 50	— 30	— 10	5	8	25	241	490	731	— 249
— 12	— 13	— 15	— 16	— 20	— 25	— 24	— 20	— 10	2	3	9	413	422	— 404
— 35	— 28	— 25	— 22	— 21	— 17	— 5	6	9	9	10	156	400	554	— 244
— 90	— 80	— 60	— 30	— 10	3	4	0	1	4	6	311	444	755	— 133
— 88	— 67	— 45	— 20	— 2	5	6	3	3	5	5	319	389	708	— 70
— 87	— 78	— 55	— 32	— 15	— 7	— 4	— 7	— 8	— 7	— 6	120	437	557	— 317
— 33	— 28	— 20	— 12	— 7	— 5	— 5	— 7	— 7	— 5	— 4	72	210	282	— 138
— 8	— 6	— 6	— 3	— 2	— 3	— 5	— 8	— 10	— 11	— 10	0	183	183	— 183
26	26	22	15	7	— 2	— 11	— 12	— 5	3	— 3	154	261	415	— 107
30	29	30	30	25	15	5	— 1	— 7	— 11	— 16	295	157	452	138
24	24	20	9	— 7	— 16	— 17	— 13	— 4	6	15	161	272	433	— 111
— 8	— 13	— 22	— 22	— 15	— 9	— 3	2	6	10	10	155	181	336	— 26
— 21	— 8	— 9	— 10	— 5	— 2	— 1	0	2	3	2	75	176	251	— 101
— 20	— 20	— 19	— 16	— 11	— 6	0	3	4	7	10	226	124	350	102
— 31	— 30	— 23	— 17	— 10	— 5	— 2	2	4	8	9	256	172	428	84
— 17	— 17	— 15	— 13	— 11	— 9	— 8	— 7	— 6	— 3	— 2	76	134	210	— 58
— 3	— 4	— 3	— 2	0	2	3	4	5	5	6	143	14	157	129

	Station	Local 12	13	14	15	16	17	18	19	20	21	22	23	24
	Range III.													
Declination.	Angmagssalik	— 8	— 5	1	9	18	27	35	40	41	39	35	30	20
	Sveagruvan	1	— 4	— 8	— 5	4	9	11	11	9	6	3	— 3	— 10
	Bear Island	6	7	7	8	10	12	12	10	8	5	2	— 2	— 10
	Tromsø	2	4	6	7	8	9	11	11	8	— 2	— 14	— 25	— 37
	Bossekop	0	2	2	2	4	7	8	8	8	2	— 15	— 37	— 39
	Petsamo	1	3	7	10	9	8	7	6	4	— 3	— 12	— 25	— 40
	Sodankylä	0	2	0	0	0	— 4	— 8	— 12	— 10	— 4	— 4	— 7	— 11
	Lerwick	1	1	1	— 3	— 6	— 11	— 14	— 17	— 19	— 20	— 20	— 18	— 16
	Lovø	— 1	1	1	1	— 1	— 4	— 7	— 13	— 16	— 18	— 19	— 20	— 19
	Rude Skov	3	4	3	2	1	— 2	— 5	— 10	— 13	— 16	— 17	— 17	— 17
Hor. Intensity.	Angmagssalik	45	60	64	50	15	— 35	— 50	— 60	— 60	— 40	— 35	— 60	— 55
	Sveagruvan	— 2	— 12	— 15	— 25	— 31	— 35	— 40	— 42	— 42	— 41	— 36	— 30	— 18
	Bear Island	40	47	54	47	22	— 10	— 40	— 70	— 80	— 80	— 80	— 78	— 75
	Tromsø	5	15	25	34	43	54	57	40	— 10	— 74	—130	—160	—172
	Bossekop	10	15	34	38	44	53	60	55	2	— 60	—110	—140	—145
	Petsamo	4	8	14	20	22	36	40	55	45	— 20	—105	—135	—126
	Sodankylä	0	2	5	6	8	17	30	40	20	— 18	— 60	— 87	— 85
	Lerwick	— 14	— 12	— 10	— 10	— 11	— 13	— 13	— 12	— 11	— 11	— 15	— 18	— 18
	Lovø	— 13	— 14	— 14	— 13	— 13	— 15	— 16	— 14	— 13	— 10	— 10	— 10	— 11
	Rude Skov	— 15	— 17	— 16	— 16	— 17	— 20	— 20	— 16	— 11	— 10	— 10	— 10	— 10
Ver. Intensity.	Angmagssalik	— 23	— 34	— 49	— 65	— 73	— 64	— 50	— 33	— 12	8	22	33	39
	Sveagruvan	— 40	— 42	— 44	— 38	— 30	— 23	— 15	— 3	— 12	23	35	40	41
	Bear Island	0	— 16	— 32	— 45	— 53	— 54	— 51	— 30	0	40	65	80	88
	Tromsø	10	15	20	21	18	12	— 3	— 20	— 27	— 25	— 2	10	4
	Bossekop	4	5	8	10	11	— 7	— 6	— 20	— 30	— 28	— 19	— 12	— 8
	Petsamo	21	23	25	26	30	31	25	11	— 4	— 13	— 18	— 21	— 22
	Sodankylä	13	16	19	22	30	40	44	35	15	— 12	— 40	— 58	— 77
	Lerwick	4	6	11	14	20	37	31	25	17	7	— 3	— 12	— 25
	Lovø	8	10	11	12	14	17	21	21	17	8	0	— 5	
	Rude Skov	5	5	6	8	10	13	16	17	13	8	3	0	
	Range IV.													
Declination.	Angmagssalik	— 20	— 16	— 3	13	30	42	51	56	60	55	43	30	16
	Sveagruvan	— 10	— 5	0	13	24	36	42	44	40	30	15	0	— 20
	Bear Island	— 3	— 2	9	15	21	26	30	31	30	18	0	— 21	— 43
	Tromsø	2	4	7	10	11	11	10	8	3	— 10	— 30	— 53	— 73
	Bossekop	6	10	16	20	20	16	13	10	0	— 12	— 26	— 52	— 80
	Petsamo	11	14	17	25	26	22	16	8	— 10	— 32	— 64	— 85	— 95
	Sodankylä	0	2	4	6	0	— 9	— 13	— 15	— 12	— 10	— 8	— 14	— 17
	Lerwick	8	9	9	6	1	— 6	— 12	— 20	— 25	— 27	— 28	— 27	— 27
	Lovø	2	8	8	4	— 2	— 10	— 22	— 30	— 32	— 29	— 25	— 22	— 18
	Rude Skov	— 2	— 1	— 2	— 3	— 6	— 9	— 12	— 13	— 14	— 16	— 17	— 16	— 13
Hor. Intensity.	Angmagssalik	51	60	40	15	— 11	— 34	— 57	— 88	—104	— 92	— 77	— 68	— 70
	Sveagruvan	16	0	— 15	— 30	— 45	— 62	— 76	— 82	— 70	— 32	— 15	— 20	— 32
	Bear Island	85	92	71	43	14	— 35	— 84	—130	—137	—117	—110	—123	—160
	Tromsø	43	50	80	96	100	81	45	0	— 60	—140	—230	—301	—326
	Bossekop	42	54	63	93	100	86	53	12	— 35	—112	—192	—280	—310
	Petsamo	25	30	40	74	94	93	70	30	— 22	— 90	—160	—220	—320
	Sodankylä	10	15	23	44	64	77	78	60	12	— 52	—130	—190	—226
	Lerwick	— 7	— 3	2	6	10	13	11	4	— 4	— 15	— 27	— 42	— 57
	Lovø	— 18	— 16	— 16	— 16	— 16	— 16	— 15	— 15	— 15	— 18	— 24	— 24	— 26
	Rude Skov	— 20	— 21	— 22	— 22	— 23	— 23	— 24	— 22	— 20	— 17	— 14	— 12	— 12

time

1	2	3	4	5	6	7	8	9	10	11	*PS*	*NS*	*AS*	*PS—NS*
7	— 3	— 9	— 13	— 15	— 14	— 10	— 4	2	— 2	— 7	304	90	394	214
— 20	— 32	— 42	— 52	— 54	— 47	— 36	— 24	— 15	— 6	— 1	54	359	413	— 305
— 23	— 35	— 47	— 55	— 50	— 33	— 13	2	6	5	5	105	268	373	— 163
— 46	— 48	— 39	— 28	— 16	— 7	— 2	1	1	0	0	68	264	321	— 196
— 45	— 46	— 40	— 31	— 21	— 8	— 1	2	2	1	0	48	283	331	— 235
— 46	— 43	— 36	— 28	— 18	— 6	0	2	3	3	1	64	257	321	— 193
— 13	— 11	— 4	— 1	0	0	0	— 1	— 1	— 1	— 1	2	93	95	— 91
— 9	— 5	— 4	— 4	— 3	— 3	— 3	— 3	— 3	— 3	— 1	3	182	185	— 179
— 17	— 14	— 5	— 3	— 3	— 4	— 3	— 3	— 3	— 3	— 2	3	178	181	— 175
— 14	— 7	— 3	— 4	— 5	— 4	— 3	— 3	— 3	— 2	0	13	145	158	— 132
— 40	— 30	— 34	— 50	— 54	— 52	— 40	— 20	4	20	30	288	695	983	— 407
— 17	— 29	— 34	— 38	— 41	— 40	— 36	— 24	— 10	— 6	— 4	0	648	648	— 648
— 76	— 70	— 70	— 72	— 60	— 25	5	17	25	31	35	323	884	1207	— 561
—160	—144	—110	— 70	— 30	— 4	5	8	7	3	3	299	1064	1363	— 765
—134	—122	—100	— 70	— 25	0	8	7	5	3	6	340	818	1158	— 478
—110	— 90	— 75	— 62	— 45	— 20	— 3	2	2	0	— 3	248	791	1039	— 543
— 73	— 61	— 54	— 40	— 23	— 7	— 1	— 1	0	— 2	— 2	128	514	642	— 386
— 22	— 19	— 17	— 13	— 11	— 10	— 10	— 11	— 13	— 15	— 16	0	329	329	— 329
— 11	— 11	— 9	— 8	— 8	— 7	— 7	— 6	— 8	— 11	— 12	0	244	244	— 244
— 9	— 9	— 9	— 10	— 9	— 10	— 10	— 9	— 12	— 13	— 14	0	302	302	— 302
42	42	40	29	14	— 10	— 23	— 25	— 17	— 10	— 15	269	504	773	— 235
44	52	56	53	36	— 15	— 4	— 15	— 23	— 28	— 35	392	355	747	37
91	90	80	55	10	— 15	— 22	— 15	— 4	2	4	605	337	942	268
— 11	— 24	— 36	— 42	— 35	— 21	— 12	— 4	4	10	10	134	262	396	— 128
— 12	— 22	— 33	— 39	— 33	— 18	— 10	— 4	1	3	2	51	294	345	— 243
— 28	— 34	— 36	— 37	— 35	— 27	— 10	3	8	12	17	232	285	517	— 53
— 79	— 70	— 56	— 40	— 26	— 15	— 5	0	4	8	10	256	478	734	— 222
— 30	— 29	— 22	— 14	— 7	— 3	0	2	1	2	3	170	148	318	22
— 9	— 11	— 12	— 10	— 5	— 2	1	3	4	5	6	158	62	220	96
— 3	— 6	— 7	— 6	— 3	— 1	0	2	3	5	5	119	28	147	91
0	— 14	— 26	— 30	— 26	— 20	— 11	— 7	— 6	— 10	— 16	395	205	600	190
— 37	— 47	— 52	— 55	— 56	— 52	— 40	— 30	— 19	— 15	— 13	244	451	695	— 207
— 62	— 80	— 90	— 94	— 85	— 65	— 30	— 3	8	8	2	198	578	776	— 380
— 87	— 96	— 95	— 80	— 46	— 18	2	6	6	5	3	88	588	676	— 500
— 97	—104	— 97	— 70	— 30	— 6	10	14	13	10	6	164	574	738	— 410
— 94	— 88	— 66	— 30	— 10	5	12	13	12	8	8	197	574	771	— 377
— 20	— 21	— 18	— 8	0	7	8	10	10	7	5	59	165	225	— 106
— 26	— 22	— 15	— 9	— 4	2	5	6	7	7	6	66	248	314	— 182
— 15	— 10	— 6	— 2	1	3	5	6	5	4	2	48	223	271	— 175
— 10	— 8	— 6	— 5	— 5	— 4	— 4	— 4	— 3	— 3	— 3	0	179	179	— 179
— 83	— 98	—114	—124	—125	—107	— 77	— 45	— 10	18	38	222	1384	1606	—1162
— 38	— 35	— 26	— 26	— 41	— 53	— 37	— 13	10	24	27	77	748	825	— 671
—172	—167	—164	—168	—150	—104	— 55	— 14	22	47	70	444	1830	2274	—1386
—320	—296	—250	—190	—110	— 55	— 15	5	10	18	26	554	2393	2947	—1839
—300	—275	—215	—150	—100	— 47	— 15	— 3	6	17	30	556	2034	2590	—1478
—340	—290	—187	—130	— 70	— 33	— 12	— 5	0	12	20	488	1879	2367	—1391
—228	—184	—140	—100	— 65	— 40	— 23	— 13	— 10	— 4	3	386	1405	1791	—1019
— 60	— 52	— 40	— 27	— 19	— 15	— 12	— 12	— 12	— 11	— 11	46	426	472	— 380
— 23	— 18	— 18	— 17	— 15	— 15	— 15	— 15	— 16	— 17	— 18	0	422	422	— 422
— 12	— 13	— 14	— 15	— 15	— 16	— 17	— 18	— 18	— 20	— 22	0	423	432	— 432

Ver. Intensity. Station	Local 12	13	14	15	16	17	18	19	20	21	22	23	24
Angmagssalik	— 56	— 72	— 97	—115	—117	— 77	— 30	5	40	72	90	100	110
Sveagruvan	— 48	— 52	— 56	— 46	— 30	— 10	13	35	54	76	94	108	116
Bear Island	— 20	— 40	— 60	— 76	— 83	— 84	— 77	— 60	— 25	45	102	140	166
Tromsø	25	28	22	10	— 10	— 37	— 63	— 72	— 62	— 25	32	47	47
Bossekop	25	27	21	9	— 6	— 20	— 36	— 48	— 51	— 43	— 12	16	27
Petsamo	26	33	36	30	23	3	— 20	— 41	— 46	— 63	— 52	— 12	18
Sodankylä	34	43	50	54	51	40	14	— 15	— 40	— 66	— 95	—116	—134
Lerwick	15	18	28	40	50	58	60	46	20	— 5	— 36	— 61	— 80
Lovø	14	16	18	22	32	38	40	33	20	4	— 12	— 26	— 37
Rude Skov	6	7	9	16	22	27	28	26	16	6	— 4	— 12	— 17
de Bilt	1	2	4	7	12	14	14	11	8	4	0	— 4	— 8

Bear Island and up to Spitzbergen, *across a geomagnetic meridian* in this region of the globe.

From table 1 it is evident that the geomagnetic meridian in question corresponds to about $\Lambda = 120°$.

In fig. 6—9 the changes of the disturbance field is demonstrated for the four ranges of storminess.

For $\triangle D$ the broken lines represent negative values, $\triangle D$ is directed *east*-wards. The full lines represent positive values, $\triangle D$ is here directed *west*-wards. The heavy broken line represents *zero*-values.

For $\triangle H$ the broken lines represent negative values, $\triangle H$ is here directed *south*-wards. The full lines represent positive values, $\triangle H$ is here directed *north*-wards. The heavy broken lines indicate *maximum* values of $\triangle H$ (either with positive or negative signs).

For $\triangle Z$ the broken lines represent negative values, $\triangle Z$ is directed *up*. The full lines represent positive values, $\triangle Z$ is here directed *down*. The heavy broken lines represent *zero*-values of $\triangle Z$.

From fig. 6—9 we see that the isopletes in $\triangle H$ and $\triangle Z$ run approximately parallel with the geomagnetic latitudes. Two periods of disturbance are present, one with maximum values at about 17^h local time with *positive* values of $\triangle H$, and the second with a maximum at about 1^h with *negative* values of $\triangle H$. In $\triangle Z$ we have a characteristic variation with negative values to the north and positive to the south during the first disturbance, and a change to the opposite during the second period of disturbance.

Assuming now that the D-field is produced by a section of a narrow linear current flowing parallel with the geomagnetic circle of latitude, it is evident that one just below the main current must have maximum values in $\triangle H$ and zero in $\triangle Z$, and a variation in $\triangle H$ and $\triangle Z$ which qualitatively is in accordance with the isoplete curves. During the afternoon disturbance, the current flows from west to east with the deflections in $\triangle Z$ negative north and positive south of the current centre, and for the midnight disturbance the current flows from east to west with the deflections in $\triangle Z$ positive north and negative south of the current centre. In the figures for $\triangle H$ and $\triangle Z$ a heavy broken line is drawn up along the region in which $\triangle H$ has maximum values, and in $\triangle Z$ the zero values are marked out by a simular broken line. These lines thus represent the horizontal projections of the movement of the current centre in the course of the day. The line on the $\triangle H$ map ought of course to coincide with the corresponding line on the $\triangle Z$ map.

In the literature the horizontal projections of the disturbing current in the polar region usually has been assumed to coincide with the zone of maximum auroral frequency. In fig. 10 a and b these „auroral zones" have been drawn up separately from the $\triangle H$ and $\triangle Z$ maps and in fig. 10 c the mean values from the $\triangle H$ and $\triangle Z$ projections are drawn up. From these figures we get the following mean values for the „auroral zone" relative to Tromsø at the hours of maximum disturbance:

time

1	2	3	4	5	6	7	8	9	10	11	*PS*	*NS*	*AS*	*PS—NS*
124	134	121	90	57	24	0	— 23	— 32	— 40	— 48	967	707	1674	260
120	117	110	102	80	54	33	12	— 7	— 26	— 38	1124	313	1437	811
170	163	154	124	72	12	— 14	— 21	— 15	— 4	— 4	1148	583	1731	565
38	7	— 42	— 74	— 83	— 68	— 48	— 23	— 2	10	20	286	609	895	— 323
22	4	— 18	— 41	— 58	— 57	— 40	— 22	— 10	8	17	176	463	639	— 287
12	— 40	— 68	— 68	— 56	— 42	— 27	— 13	— 3	9	18	208	552	760	— 344
—137	—132	—112	— 91	— 71	— 50	— 29	— 8	6	16	25	333	1096	1429	— 763
— 90	— 90	— 75	— 60	— 46	— 32	— 20	— 10	— 2	6	11	352	607	959	— 255
— 42	— 43	— 39	— 32	— 24	— 16	— 9	— 3	2	7	10	256	283	539	— 27
— 22	— 24	— 24	— 20	— 16	— 11	— 8	— 3	2	5	6	176	161	337	15
— 11	— 11	— 10	— 8	— 6	— 4	— 3	— 1	0	1	1	79	66	145	13

Table 5.

Range	Afternoon maximum at 17h	Midnight maximum at 24h	Afternoon maximum at 17h	Midnight maximum at 24h
	Geomagnetic latitudes		Distance from Tromø	
I ...	—	69°.0	—	200 km north
II ...	67°.4	67°.5	33 km north	44 » »
III ...	66°.5	67°.1	67 » south	0 »
IV ...	65°.8	65°.8	176 » »	143 » south

From table 5 we see that the „auroral zone" during the maximum phases for very small disturbances, range I, lies north of Tromsø at a distance of about 200 km. For small to medium storms, range II, the „auroral zone" during the maximum phases lies about 40 km north of Tromsø. For stronger storms, range III, the „auroral zone" lies roughly over Tromsø, and for the strongest storms, range IV, the „auroral zone" moves further south and lies about 160 km south of Tromsø.

This corresponds fairly well with the actual appearance of the aurorae. The year 1932—33 was a minimum year during which the storms of range III and IV did not attain the very highest values. The aurorae also did not appear over Middle Europe, as frequently may be the case during maximum years. The great aurorae during this winter, which on lower latitudes were carefully observed by Størmer, were only restricted to appear over Southern Norway.

The most interesting detail of the „auroral zones" deduced from the *D*-fields, is the *discontinuity* between the afternoon and the midnight sections. As previously mentioned, there appears in the diurnal curves of S_D in Z a double wave at the stations where Φ lies in the range 65°—70°. This double wave is in fact produced by the successive passages of the „negative" and „positive" sections of the auroral zones across the geomagnetic meridian in the course of the day. It would be of the greatest interest if it could be decided whether there is a parallel discontinuity in the mean appearance and movement of the aurorae. From our general experience on auroral watch during more than fifteen winters, we have impression that in the dark winter period the aurorae appear with great intensity already in the afternoon at 17h—18h, then there is a quiet period and the next great period of auroral activity starts at about 21h local time. This question must, however, be more closely examined by objective registrations of the luminosity. A suitable apparatus for recording auroral luminosity on the northern sky, in zenith and on the southern sky independently and simultaneously, is described in section II.

An interesting question is to what extent the fig. s. 6—9 may be assumed to represent the mean fields of disturbance around the whole polar region. As previously stressed, the maps represent the changes in the *D*-field in the course of a day across the 120° geomagnetic meridian. If it is to be assumed that the effect of the diurnal rotation of the earth is simply to displace the *D*-field along the geomagnetic latitude circles, fig. s. 6—9 will also give the mean disturbance field over the whole polar region. There is cer-

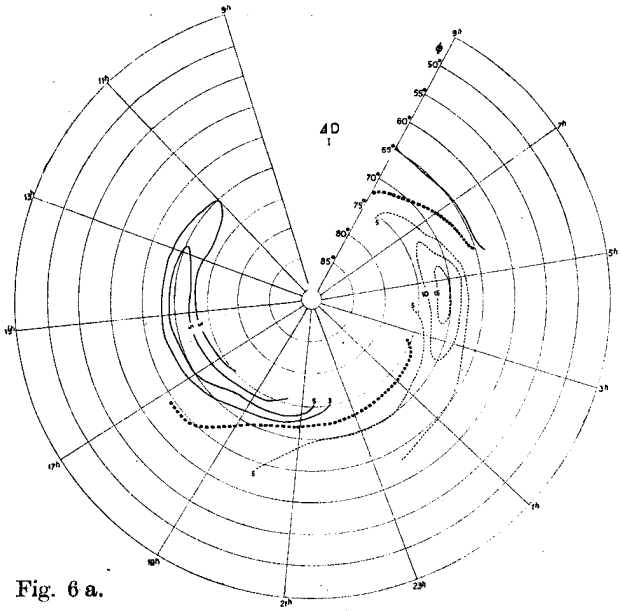

Fig. 6 a.

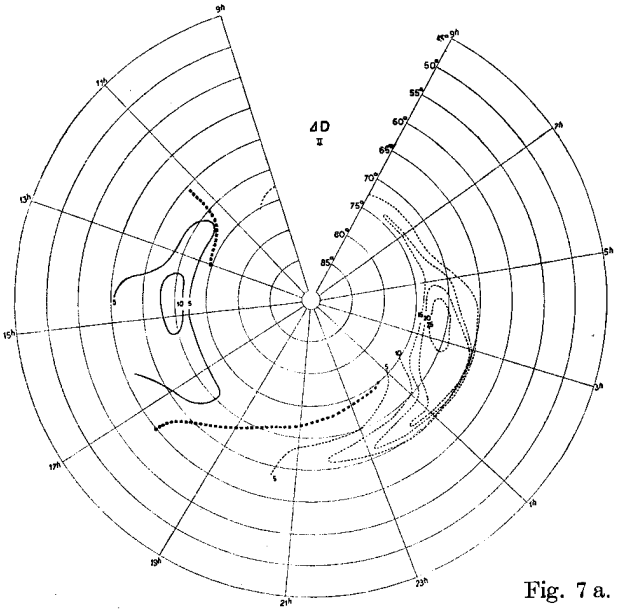

Fig. 7 a.

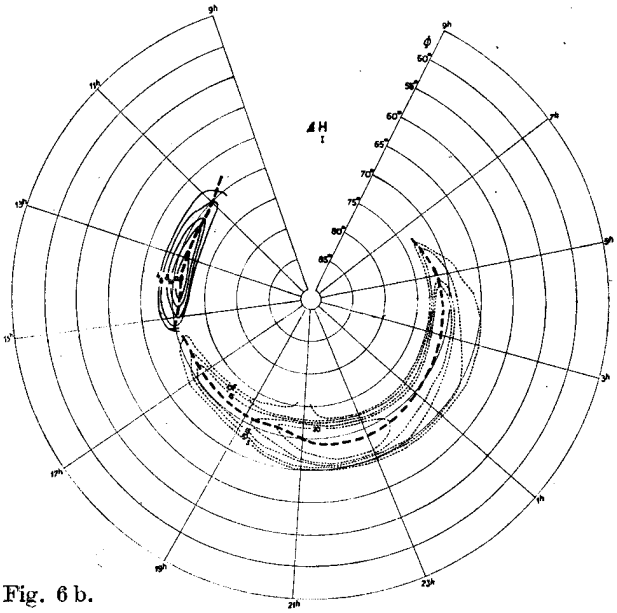

Fig. 6 b.

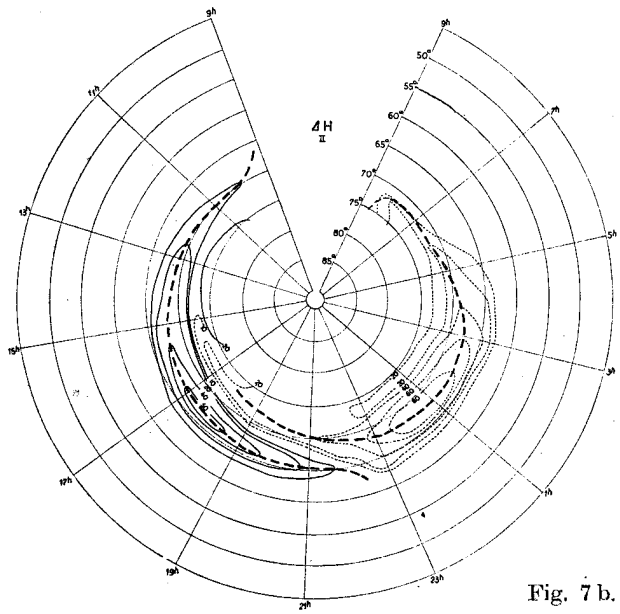

Fig. 7 b.

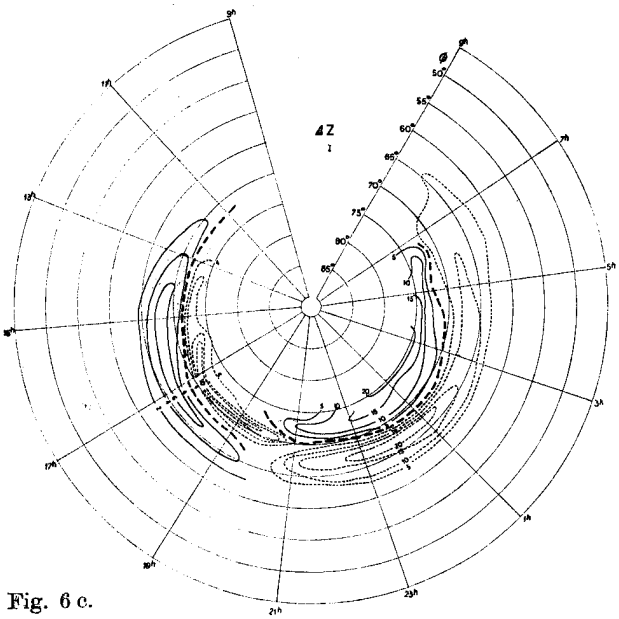

Fig. 6 c.

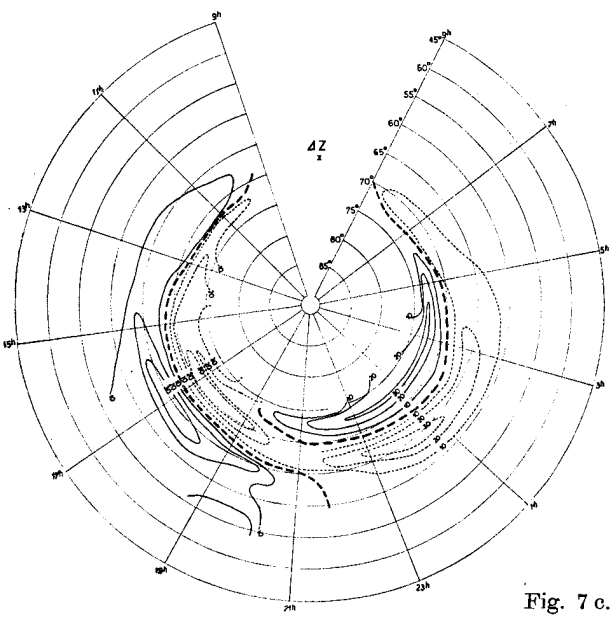

Fig. 7 c.

Fig. 6 a, b and c. Variation of the three components ($\triangle D$, $\triangle H$ and $\triangle Z$) of the D-field with local time across the 120° geomagnetic meridian. *Range I.*

Fig. 7 a, b and c. Variation of the three components ($\triangle D$, $\triangle H$ and $\triangle Z$) of the D-field with local time across the 120° geomagnetic meridian. *Range II.*

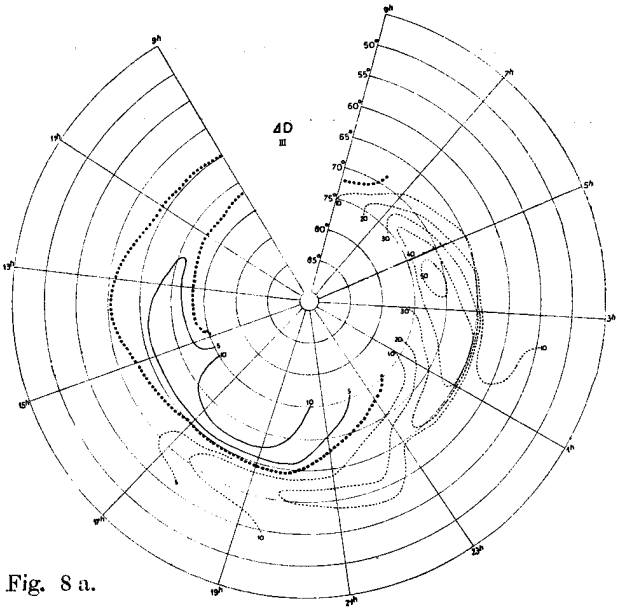

Fig. 8 a.

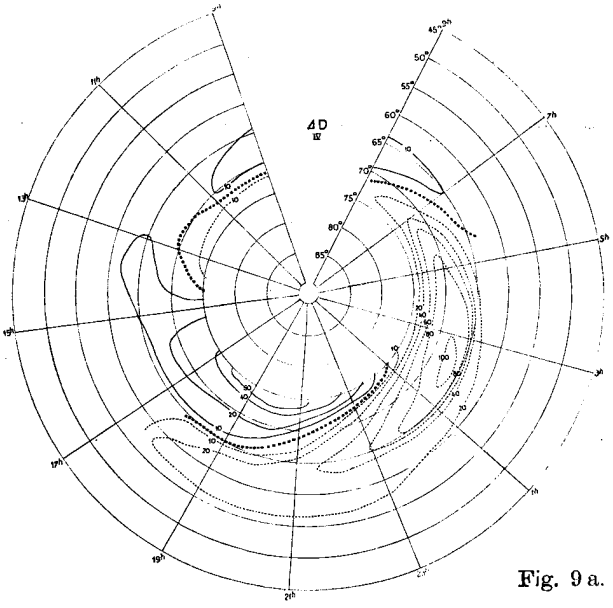

Fig. 9 a.

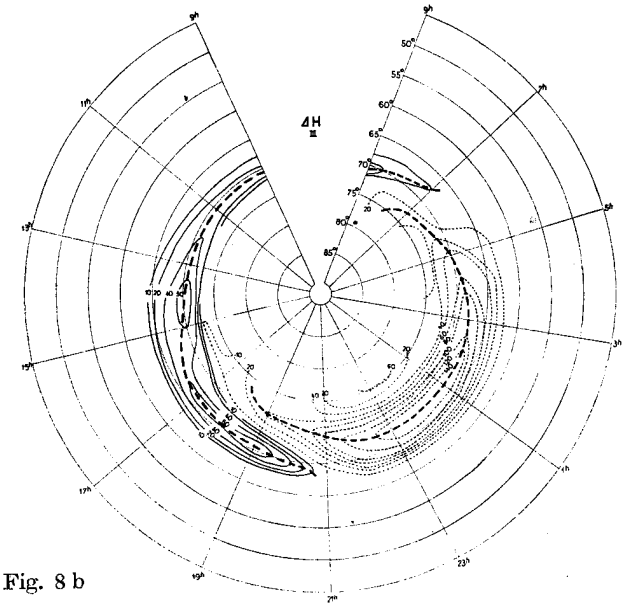

Fig. 8 b

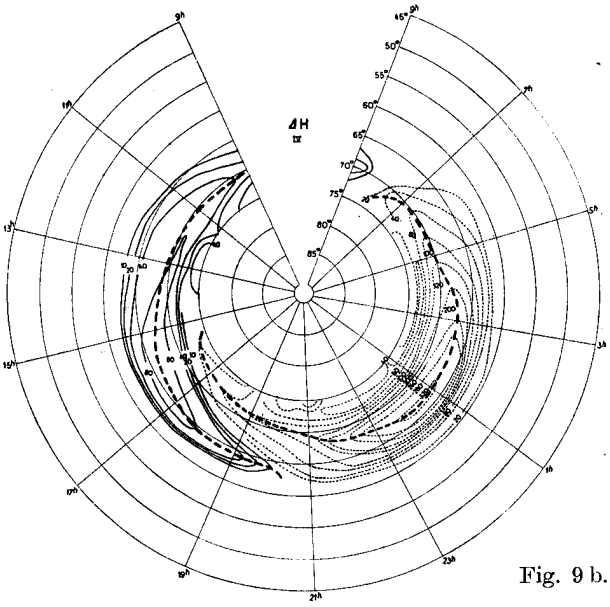

Fig. 9 b.

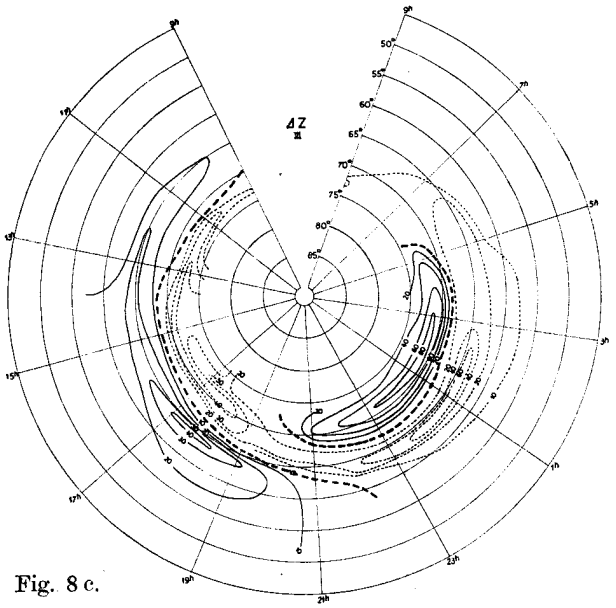

Fig. 8 c.

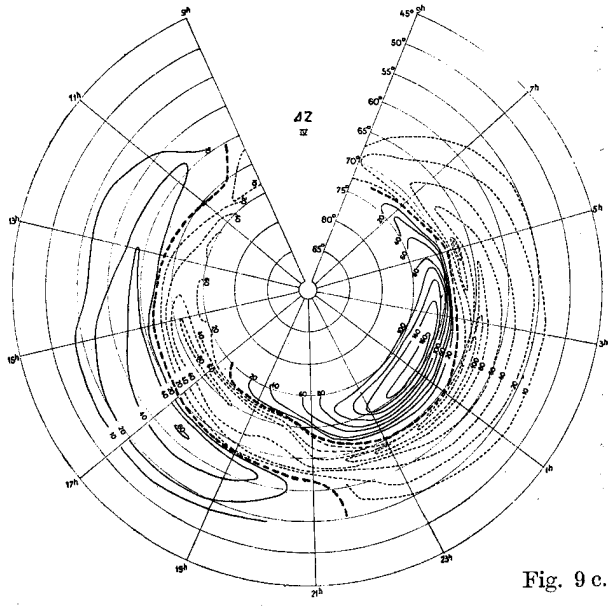

Fig. 9 c.

Fig. 8 a, b and c. Variation of the three components ($\triangle D$, $\triangle H$ and $\triangle Z$) of the D-field with local time across the 120° geomagnetic meridian. *Range III.*

Fig. 9 a, b and c. Variation of the three components ($\triangle D$, $\triangle H$ and $\triangle Z$) of the D-field with local time across the 120° geomagnetic meridian. *Range IV.*

Table 4. Mean diurnal variation of Storminess (S_D)
Polar Year

	Φ	Local 12	13	14	15	16	17	18	19	20	21	22
						Range I.						
Declination.	75											
	74	3	2	1	2	3	4	5	6	6	5	3
	73	3	3	4	4	4	5	5	6	6	2	1
	72	4	4	5	5	5	5	4	4	5	0	— 1
	71	4	4	5	6	6	5	4	2	— 1	— 2	— 2
	70	4	5	6	6	6	5	3	1	— 2	— 3	— 5
	69	3	4	5	5	4	3	2	0	— 2	— 5	— 7
	68	2	3	3	3	3	2	1	— 1	— 3	— 5	— 8
	67	2	2	2	2	2	2	1	— 1	— 3	— 6	— 8
	66	2	2	2	2	2	2	1	— 1	— 3	— 6	— 7
	65	2	2	3	3	3	3	1	— 1	— 3	— 6	— 7
	64	1	1	0	— 3	— 4	— 4	— 5	— 6	— 6	— 9	— 9
	63	— 1	— 1	0								
Hor. Intensity.	75	13						6	2	— 1	— 7	— 7
	74	10	15	18	17	11	6	0	— 4	— 8	— 8	— 6
	73	5	6	7	2	— 1	— 5	— 9	— 11	— 10	— 8	— 6
	72	8	11	12	4	— 5	— 15	— 16	— 17	— 21	— 21	— 19
	71	11	14	15	8	— 8	— 18	— 20	— 21	— 24	— 28	— 29
	70	9	11	11	8	— 8	— 16	— 18	— 19	— 23	— 29	— 29
	69	7	7	7	6	— 3	— 8	— 9	— 14	— 20	— 28	— 29
	68	4	4	4	4	2	0	3	— 3	— 17	— 25	— 29
	67	1	2	2	2	4	8	10	4	— 14	— 21	— 28
	66	1	0	0	0	4	7	8	5	— 4	— 13	— 22
	65	1	0	— 1	— 1	0	3	4	5	3	— 2	— 7
	64	0	0	0	— 1	0	1	3	3	4	3	1
	63	0	0	0	0	0	1	1	1	4	5	4
	62							0	0	4	0	
Ver. Intensity.	75	4	3	3	0	— 6	— 11	— 12	— 13	— 12		
	74	2	0	— 2	— 5	— 8	— 10	— 9	— 10	— 8	— 11	8
	73	— 1	— 4	— 12	— 12	— 10	— 8	— 7	— 3	1	11	14
	72	0	— 2	— 1	— 6	— 8	— 8	— 9	— 6	— 1	8	12
	71	2	4	5	4	— 2	— 10	— 11	— 12	— 12	1	5
	70	3	4	6	5	3	— 4	— 6	— 6	— 9	— 4	— 3
	69	2	3	6	6	5	0	— 1	— 3	— 5	— 7	— 10
	68	1	2	5	6	7	4	3	1	— 2	— 11	— 16
	67	1	2	4	6	7	6	6	4	0	— 13	— 18
	66	0	1	3	6	6	6	6	5	2	— 11	— 15
	65	— 1	0	2	3	4	4	5	5	3	— 5	— 10
	64	— 2	0	0	1	2	3	3	3	2	— 5	— 10
	63	— 1	0	0	1	2	2	2	2	2	1	— 2
	62	0	0	1	1	2	2	2	3	3	4	2
						Range II.						
Declination.	74	2	— 2	— 4	— 5	— 1	1	4	5	5	7	3
	73	6	5	3	0	2	3	4	4	4	2	0
	72	7	8	9	6	5	5	4	2	2	0	— 2
	71	7	9	12	11	8	6	5	0	0	— 1	— 2
	70	6	7	12	12	9	7	4	0	— 1	— 2	— 3
	69	4	4	11	12	8	6	4	0	— 1	— 4	— 6

in gammas for varying geomagnetic latitudes Φ.

1932—33.

time												
23	24	1	2	3	4	5	6	7	8	9	10	11
2	3	1	0	— 2	— 7	— 11	— 10	— 9	— 5	— 2	0	2
0	— 1	— 2	— 3	— 8	— 11	— 13	— 12	— 9	— 5	— 1	0	2
— 2	— 2	— 4	— 5	— 13	— 15	— 15	— 12	— 7	— 2	— 1	0	2
— 3	— 3	— 5	— 7	— 15	— 17	— 17	— 10	— 4	— 1	2	2	2
— 5	— 5	— 6	— 8	— 14	— 15	— 15	— 8	— 3	0	2	2	3
— 7	— 7	— 7	— 8	— 11	— 12	— 12	— 5	— 1	1	2	2	2
— 8	— 9	— 8	— 7	— 8	— 8	— 9	— 2	0	1	1	1	2
— 9	— 10	— 9	— 7	— 5	— 4	— 3	— 1	1	2	1	1	2
— 8	— 8	— 7	— 6	— 4	— 3	— 2	0	1	3	1	1	1
— 7	— 7	— 5	— 5	— 3	— 2	— 1	1	2	5	2	2	2
— 8	— 6	— 4	— 3	1	2	4	6	9	9	5	3	0
— 1	8							0	0			
— 1	5	12	17	18	14	8	2	— 1	— 1	1	4	6
— 2	0	2	— 1	— 4	— 8	— 10	— 10	— 8	— 4	— 1	2	4
— 12	— 10	— 10	— 14	— 21	— 24	— 12	— 7	— 2	— 2	0	3	5
— 26	— 20	— 20	— 26	— 32	— 28	— 12	0	2	4	1	2	7
— 28	— 21	— 20	— 25	— 28	— 21	— 11	2	3	5	2	2	6
— 28	— 23	— 20	— 24	— 19	— 12	— 7	2	3	4	2	2	5
— 28	— 24	— 18	— 17	— 12	— 7	— 4	2	3	3	2	2	4
— 27	— 21	— 17	— 13	— 8	— 4	— 2	1	2	2	1	1	3
— 25	— 18	— 16	— 12	— 8	— 5	— 2	— 1	0	0	0	0	1
— 12	— 15	— 15	— 10	— 8	— 6	— 4	— 2	— 2	— 1	— 1	0	0
— 2	— 6	— 6	— 5	— 4	— 3	— 2	— 2	0	2	1	1	1
3	0	0	0				— 1	2				
11	20	22	22	21	18	16	6	7	4	2	2	4
13	18	19	19	18	14	10	11	4	3	1	1	3
16	16	13	11	10	6	4	14	0	1	0	1	2
14	13	12	10	8	4	— 1	2	— 4	— 3	— 2	0	0
8	11	11	10	5	1	— 3	— 5	— 8	— 8	— 4	— 2	1
0	6	8	6	0	— 2	— 6	— 8	— 9	— 8	— 4	— 2	1
— 7	— 2	0	2	— 6	— 6	— 9	— 9	— 9	— 6	— 3	— 1	0
— 16	— 16	— 8	— 8	— 10	— 10	— 11	— 10	— 8	— 4	— 2	— 1	0
— 22	— 22	— 21	— 14	— 11	— 9	— 10	— 10	— 8	— 4	— 1	0	0
— 19	— 20	— 20	— 16	— 12	— 9	— 7	— 9	— 8	— 4	— 2	— 1	— 1
— 13	— 15	— 16	— 15	— 13	— 10	— 9	— 8	— 8	— 5	— 3	— 2	— 1
— 13	— 14	— 14	— 14	— 9	— 9	— 9	— 8	— 8	— 5	— 3	— 3	— 2
— 7	— 6	— 6	— 6	— 1	— 1	— 1	— 7	— 5	— 3	— 3	— 3	— 2
2	2	2	2	2	2	2	— 2	— 2	— 2	— 2	— 2	— 1
0	0	— 7	— 14	— 15	— 15	— 11	— 15	— 15	— 15	— 12	— 8	— 3
— 2	— 5	— 7	— 18	— 22	— 22	— 16	— 15	— 14	— 14	— 11	— 8	— 3
— 3	— 5	— 10	— 20	— 26	— 26	— 17	— 12	— 10	— 10	— 7	— 6	— 4
— 3	— 5	— 8	— 20	— 28	— 27	— 18	— 7	2	3	— 3	— 4	— 4
— 5	— 7	— 10	— 20	— 27	— 26	— 16	— 3	4	4	— 3	— 4	— 3
— 8	— 11	— 13	— 21	— 25	— 20	— 12	— 1	4	4	— 3	— 3	— 2

	Φ	Local 12	13	14	15	16	17	18	19	20	21	22
Declination.	68	2	4	10	10	8	6	4	0	— 2	— 6	— 8
	67	1	4	8	9	8	5	3	1	— 3	— 7	— 10
	66	1	3	5	7	7	7	5	2	0	— 5	— 11
	65	1	1	5	9	9	9	12	10	2	9	— 3
	64	2	2	5	8	7	4	— 2	— 5	— 7	— 9	— 8
	63	3	3	6	7	6	3	— 1	— 5	— 7	— 7	— 8
	62	5	5	7	6	6	3	3	— 2	— 4	— 6	— 8
Hor. Intensity.	75	50	60	60	45	35	15	— 10	— 28	— 34	— 28	— 24
	74	45	48	48	31	14	2	— 18	— 27	— 29	— 25	— 22
	73	5	3	— 2	— 18	— 30	— 37	— 36	— 27	— 22	— 24	— 22
	72	7	7	3	— 8	— 12	— 20	— 28	— 28	— 23	— 23	— 21
	71	14	23	30	25	20	6	— 10	— 25	— 32	— 40	— 43
	70	16	27	34	33	30	25	6	— 15	— 20	— 39	— 45
	69	14	25	30	32	37	38	25	6	— 3	— 22	— 42
	68	11	18	23	30	41	49	41	25	15	— 2	— 37
	67	6	10	16	36	43	56	55	44	30	8	— 28
	66	1	5	10	19	27	48	52	47	32	13	— 15
	65	— 6	— 3	1	5	9	21	27	28	23	15	0
	64	— 5	— 4	— 2	0	4	11	16	17	16	12	— 2
	63	— 6	— 6	— 4	— 4	— 4	0	— 3	— 3	2	3	— 7
	62	— 10	— 8	— 8	— 8	— 10	— 15	— 17	— 12	— 12	— 10	— 9
Ver. Intensity.	75	— 4	— 15	— 23	— 38	— 45	— 45	— 35	— 30	— 22	— 5	2
	74	— 11	— 20	— 27	— 32	— 32	— 32	— 26	— 18	— 12	4	12
	73	— 18	— 22	— 28	— 25	— 16	— 8	1	7	12	19	26
	72	— 9	— 16	— 25	— 24	— 20	— 20	— 20	— 8	3	15	24
	71	16	1	— 15	— 24	— 34	— 47	— 42	— 30	— 15	2	11
	70	20	16	— 7	— 16	— 28	— 36	— 37	— 31	— 18	— 4	1
	69	19	9	3	— 5	— 13	— 17	— 19	— 23	— 20	— 8	— 8
	68	16	11	10	5	— 2	— 2	0	— 10	— 18	— 19	— 17
	67	10	12	12	15	12	12	12	0	— 13	— 15	— 24
	66	7	7	11	18	21	28	20	11	0	— 14	— 25
	65	12	13	17	21	30	34	30	22	12	2	— 5
	64	10	12	17	24	32	35	36	21	20	9	— 4
	63	4	4	8	17	20	26	32	20	12	6	— 3
	62	— 3	— 3	0	9	11	13	21	12	7	3	— 3
	61	— 2	— 1	2	10	11	11	21	11	8	3	— 2
	60	— 1	0	4	10	11	12	16	13	10	3	0
	59	0	2	6	9	10	12	16	16	14	6	3
	58	3	4	7	9	10	13	16	18	18	11	6
	57	5	6	7	9	10	13	16	20	21	15	10

Range III.

Declination.	74	— 3	— 3	— 4	2	8	11	14	12	11	8	5
	73	0	0	0	4	9	11	13	12	11	7	4
	72	3	3	4	7	10	11	12	11	10	7	3
	71	5	6	7	9	10	11	12	11	9	6	2
	70	5	6	8	9	9	11	12	11	9	4	— 1
	69	4	6	8	9	9	10	12	11	9	2	— 5
	68	3	5	7	8	8	10	11	10	9	0	— 10
	67	2	4	6	6	7	9	10	9	8	— 2	— 13
	66	2	3	5	5	5	6	7	6	6	— 4	— 14
	65	1	2	3	3	3	3	2	3	3	— 5	— 13
	64	0	1	3	1	0	— 2	— 5	— 6	— 7	— 10	— 13
	63	0	1	2	0	— 1	— 6	— 11	— 13	— 16	— 16	— 16
	62	0	0	1	— 1	— 3	— 8	— 14	— 17	— 20	— 20	— 19

time

23	24	1	2	3	4	5	6	7	8	9	10	11
— 12	— 15	— 17	— 21	— 20	— 14	— 7	1	4	4	— 4	— 3	— 2
— 13	— 18	— 19	— 20	— 18	— 10	— 4	2	4	4	— 4	— 3	— 2
— 15	— 18	— 22	— 23	— 21	— 12	— 4	2	4	4	— 4	— 2	— 1
— 5	— 12	— 17	— 23	— 21	— 12	— 4	2	3	3	— 3	— 3	— 3
— 7	— 6	— 3	— 2	— 2	— 1	0	3	4	4	— 5	— 5	— 3
— 9	— 6	— 3	— 2	0	— 1	0	3	5	5	— 5	— 5	— 5
— 7	— 5	— 4	— 1	0	0	0	3	5	5	— 5	— 5	— 5
— 26	— 27	— 30	— 42	— 58	— 71	— 68	— 57	— 36	— 11	12	15	30
— 21	— 15	— 15	— 15	— 45	— 60	— 60	— 47	— 20	— 15	2	8	17
— 16	— 20	— 18	— 15	— 16	— 16	— 20	— 28	— 25	— 18	— 7	2	3
— 17	— 44	— 38	— 30	— 13	— 13	— 14	— 20	— 17	— 10	— 5	4	5
— 46	— 65	— 55	— 50	— 25	— 21	— 21	— 17	— 6	4	8	9	10
— 57	— 80	— 73	— 63	— 38	— 27	— 23	— 11	— 1	5	10	10	10
— 63	— 83	— 88	— 73	— 48	— 30	— 21	— 5	1	5	8	9	10
— 63	— 85	— 90	— 78	— 56	— 29	— 17	— 1	2	4	4	5	7
— 60	— 83	— 88	— 78	— 58	— 27	— 12	3	2	1	2	4	7
— 52	— 80	— 86	— 78	— 56	— 27	— 10	— 4	— 3	— 6	— 6	— 5	— 4
— 42	— 48	— 55	— 35	— 45	— 27	— 10	— 4	— 3	— 6	— 6	— 5	— 4
— 30	— 17	— 15	— 13	— 25	— 15	— 8	— 5	— 5	— 6	— 7	— 5	— 4
— 17	— 7	— 5	— 3	— 11	— 5	— 4	— 4	— 5	— 8	— 9	— 8	— 7
— 6	— 6	— 5	— 5	— 4	— 2	— 2	— 4	— 5	— 8	— 10	— 10	— 10
12	20	21	21	19	7	0	— 7	— 14	— 15	— 4	1	7
22	26	27	27	23	17	8	0	— 10	— 11	— 5	0	— 5
30	30	30	30	30	30	24	14	4	— 3	— 7	— 10	— 14
27	27	28	28	28	22	15	5	— 4	— 6	— 8	— 10	— 10
18	20	23	23	20	8	— 5	— 15	— 16	— 13	— 5	5	12
8	11	14	17	10	— 12	— 12	— 18	— 19	— 14	— 1	8	16
— 6	0	7	9	— 1	— 8	— 14	— 17	— 17	— 12	3	9	15
— 12	— 10	— 3	2	— 10	— 15	— 13	— 13	— 9	— 6	5	10	13
— 30	— 23	— 15	— 6	— 18	— 18	— 12	— 9	— 3	0	6	10	10
— 32	— 30	— 23	— 14	— 23	— 18	— 12	— 6	1	3	6	8	10
— 18	— 32	— 28	— 22	— 23	— 18	— 11	— 5	2	4	5	7	10
— 14	— 32	— 32	— 26	— 22	— 17	— 10	— 5	0	2	3	8	10
— 10	— 20	— 25	— 25	— 17	— 15	— 10	— 7	— 4	— 3	— 2	2	4
— 8	— 12	— 14	— 14	— 14	— 12	— 9	— 9	— 7	— 5	— 6	— 3	— 3
— 6	— 8	— 11	— 11	— 11	— 8	— 6	— 7	— 5	— 3	— 3	— 2	— 2
— 5	— 6	— 8	— 8	— 7	— 6	— 4	— 3	— 2	0	0	2	2
— 2	— 3	— 5	— 5	— 5	— 3	— 2	— 2	— 2	— 2	3	3	3
2	— 2	— 3	— 4	— 4	— 2	0	— 5	— 5	— 6	5	5	5
2	— 2	— 13	— 25	— 33	— 41	— 40	— 39	— 27	— 16	— 10	— 4	— 3
— 2	— 7	— 19	— 31	— 40	— 50	— 46	— 42	— 28	— 15	— 8	— 2	— 1
— 2	— 8	— 20	— 33	— 44	— 54	— 46	— 38	— 22	— 7	— 2	2	2
— 5	— 12	— 25	— 37	— 45	— 54	— 44	— 33	— 16	1	2	4	4
— 9	— 17	— 28	— 40	— 46	— 52	— 40	— 28	— 14	1	2	4	4
— 14	— 23	— 33	— 44	— 44	— 44	— 32	— 20	— 10	1	2	3	4
— 20	— 30	— 38	— 47	— 42	— 36	— 25	— 13	— 5	2	2	2	2
— 25	— 36	— 42	— 48	— 40	— 31	— 20	— 9	— 3	2	2	2	2
— 26	— 39	— 43	— 47	— 38	— 29	— 18	— 7	— 2	2	2	2	2
— 25	— 38	— 40	— 43	— 35	— 26	— 16	— 6	— 2	2	2	2	1
— 17	— 22	— 18	— 15	— 10	— 5	— 4	— 3	— 2	— 1	— 1	0	0
— 16	— 16	— 11	— 6	— 5	— 3	— 3	— 2	— 2	— 3	— 2	— 2	— 1
— 18	— 16	— 11	— 6	— 5	— 4	— 3	— 3	— 3	— 3	— 3	— 3	— 1

	Φ	Local 12	13	14	15	16	17	18	19	20	21	22
Declination.	61	— 1	0	1	— 1	— 3	— 8	— 14	— 18	— 23	— 21	— 20
	60	— 1	0	0	— 1	— 3	— 7	— 12	— 17	— 22	— 21	— 21
	59	— 1	0	0	— 1	— 3	— 7	— 10	— 15	— 19	— 20	— 20
	58	— 1	0	1	0	— 2	— 4	— 7	— 12	— 17	— 18	— 20
	57	0	1	2	1	0	— 2	— 5	— 10	— 15	— 17	— 19
	56	2	2	3	2	1	— 2	— 5	— 9	— 13	— 15	— 17
	55	3	4	5	3	2	— 1	— 5	— 9	— 13	— 14	— 15
Hor. Intensity.	75	53	68	75	60	30	— 35	— 55	— 65	— 65	— 40	— 35
	74	40	55	60	35	5	— 35	— 48	— 56	— 56	— 40	— 35
	73	— 5	— 5	— 5	— 22	— 28	— 33	— 42	— 55	— 55	— 42	— 36
	72	30	35	44	17	— 5	— 23	— 39	— 55	— 58	— 55	— 51
	71	40	47	54	46	22	— 10	— 37	— 65	— 75	— 80	— 80
	70	38	47	55	50	30	10	— 27	— 50	— 63	— 95	—102
	69	30	38	50	47	36	25	— 6	— 25	— 45	—140	—125
	68	18	27	44	40	40	40	30	13	— 27	— 88	—134
	67	10	16	36	36	43	52	57	45	— 7	— 73	—130
	66	7	10	26	30	43	52	55	57	20	— 47	—114
	65	4	8	15	20	25	40	41	55	43	— 23	—100
	64	0	4	6	8	10	20	30	40	35	— 18	— 65
	63	— 8	— 6	— 4	— 3	— 3	— 3	5	10	0	— 14	— 28
	62	— 14	— 13	— 12	— 11	— 13	— 14	— 17	— 15	— 15	— 11	— 14
	61	— 14	— 14	— 14	— 12	— 14	— 15	— 19	— 17	— 17	— 10	— 11
	60	— 14	— 14	— 14	— 13	— 15	— 15	— 19	— 17	— 17	— 10	— 10
	59	— 14	— 14	— 14	— 13	— 15	— 15	— 17	— 15	— 15	— 10	— 10
	58	— 14	— 14	— 14	— 13	— 13	— 15	— 17	— 14	— 14	— 10	— 10
	57	— 15	— 15	— 15	— 14	— 15	— 16	— 17	— 15	— 15	— 10	— 10
	56	— 15	— 15	— 15	— 16	— 16	— 19	— 20	— 16	— 13	— 10	— 10
Ver. Intensity.	75	— 16	— 30	— 50	— 78	— 84	— 78	— 58	— 42	— 25	0	14
	74	— 25	— 35	— 48	— 57	— 64	— 57	— 45	— 26	— 8	10	24
	73	— 38	— 42	— 45	— 41	— 33	— 26	— 17	— 6	10	22	35
	72	— 25	— 35	— 41	— 41	— 35	— 31	— 30	— 9	8	33	52
	71	0	— 15	— 32	— 42	— 47	— 47	— 51	— 30	0	41	65
	70	4	— 5	— 20	— 30	— 37	— 37	— 46	— 33	— 6	40	56
	69	7	3	— 6	— 14	— 15	— 17	— 37	— 32	— 12	20	37
	68	9	9	8	6	4	— 4	— 33	— 37	— 20	— 6	15
	67	10	13	19	15	17	7	— 8	— 20	— 27	— 25	— 10
	66	6	8	14	21	25	19	7	— 8	— 26	— 27	— 24
	65	20	22	24	25	28	30	24	8	7	— 16	— 32
	64	15	18	21	23	30	38	43	30	10	— 10	— 38
	63	8	10	15	18	25	34	37	30	17	0	— 22
	62	5	6	11	16	18	25	28	25	17	8	— 2
	61	5	5	10	13	17	22	25	23	17	8	0
	60	8	8	10	13	16	20	23	23	17	8	0
	59	8	8	11	13	15	19	22	22	17	8	0
	58	8	100	11	12	14	17	21	21	17	8	1
	57	7	9	9	10	13	15	19	19	15	7	2
	56	6	7	7	8	11	13	17	17	14	7	2
						Range IV.						
Declination.	74	— 18	— 14	— 3	13	30	41	50	54	58	53	40
	73	— 10	— 5	2	13	26	38	42	44	48	35	20
	72	— 7	— 3	5	14	24	36	35	35	40	25	7
	71	— 2	— 1	8	15	21	32	29	29	29	15	— 2
	70	0	0	8	15	18	26	23	23	23	7	— 10
	69	1	2	8	15	15	23	18	16	16	0	— 20

time

23	24	1	2	3	4	5	6	7	8	9	10	11
— 19	— 17	— 12	— 7	— 6	— 5	— 4	— 4	— 4	— 4	— 3	— 3	— 2
— 20	— 19	— 14	— 10	— 7	— 5	— 4	— 4	— 4	— 4	— 3	— 3	— 2
— 20	— 19	— 15	— 12	— 8	— 4	— 4	— 4	— 4	— 3	— 3	— 3	— 2
— 20	— 20	— 16	— 13	— 8	— 4	— 4	— 4	— 4	— 3	— 3	— 3	— 2
— 19	— 19	— 15	— 10	— 6	— 3	— 3	— 4	— 3	— 3	— 3	— 3	— 1
— 18	— 19	— 13	— 8	— 6	— 4	— 4	— 5	— 4	— 3	— 2	— 2	0
— 16	— 17	— 12	— 6	— 5	— 4	— 4	— 4	— 3	— 2	— 2	— 2	— 0
— 67	— 60	— 45	— 34	— 32	— 53	— 57	— 58	— 44	— 16	12	27	27
— 55	— 48	— 36	— 27	— 33	— 47	— 50	— 50	— 38	— 20	0	15	15
— 32	— 22	— 22	— 22	— 35	— 40	— 42	— 42	— 34	— 22	— 8	— 5	— 5
— 46	— 45	— 45	— 36	— 48	— 52	— 43	— 33	— 20	— 5	5	15	20
— 80	— 76	— 76	— 70	— 70	— 70	— 60	— 25	4	15	26	40	33
—110	—110	—108	— 95	— 90	— 85	— 66	— 17	11	19	24	27	29
—135	—138	—134	—114	—105	— 86	— 65	— 12	10	18	17	18	21
—160	—160	—153	—135	—112	— 81	— 45	— 7	10	14	10	11	11
—157	—167	—158	—141	—108	— 73	— 33	— 3	6	8	6	4	4
—140	—140	—135	—111	— 92	— 68	— 26	— 3	4	5	4	2	0
—134	—125	—110	— 90	— 75	— 60	— 24	— 16	— 3	2	2	0	— 2
—100	— 92	— 80	— 67	— 56	— 42	— 22	— 10	— 2	0	0	— 2	— 3
— 40	— 40	— 35	— 30	— 31	— 20	— 15	— 8	— 6	— 6	— 9	— 12	— 12
— 16	— 18	— 18	— 20	— 15	— 12	— 11	— 11	— 10	— 10	— 13	— 15	— 15
— 12	— 14	— 14	— 17	— 12	— 10	— 10	— 11	— 10	— 10	— 13	— 15	— 15
— 10	— 13	— 13	— 14	— 11	— 10	— 10	— 10	— 8	— 8	— 12	— 14	— 14
— 10	— 12	— 12	— 13	— 9	— 9	— 9	— 8	— 8	— 8	— 10	— 13	— 13
— 10	— 11	— 11	— 11	— 9	— 9	— 9	— 7	— 7	— 7	— 9	— 12	— 13
— 10	— 10	— 10	— 10	— 9	— 9	— 9	— 7	— 7	— 7	— 10	— 12	— 13
— 10	— 9	— 9	— 9	— 9	— 10	— 9	— 8	— 8	— 8	— 12	— 13	— 14
25	37	37	37	26	16	4	— 6	— 28	— 28	— 12	— 3	— 3
33	38	42	43	22	34	17	— 11	— 18	— 24	— 18	— 16	— 20
45	42	44	51	55	52	34	— 15	— 5	— 15	— 22	— 28	— 34
63	70	70	75	70	57	25	— 15	— 10	— 15	— 14	— 17	— 23
78	88	90	90	80	55	7	— 16	— 21	— 15	— 4	2	4
73	78	75	67	70	40	— 7	— 17	— 22	— 13	1	5	7
54	54	42	30	35	13	— 20	— 18	— 18	— 10	3	6	9
28	26	11	— 5	— 12	— 23	— 29	— 20	— 15	— 7	4	8	10
5	2	— 7	— 21	— 34	— 35	— 41	— 22	— 12	— 5	5	10	10
— 17	— 15	— 18	— 35	— 35	— 35	— 38	— 24	— 10	— 3	7	12	13
— 25	— 25	— 28	— 30	— 37	— 35	— 35	— 26	— 10	3	8	12	16
— 50	— 70	— 74	— 68	— 34	— 38	— 30	— 18	— 6	2	5	9	12
— 50	— 67	— 55	— 55	— 35	— 25	— 13	— 7	— 1	2	2	4	6
— 12	— 21	— 24	— 25	— 19	— 13	— 7	— 3	0	2	1	2	4
— 8	— 16	— 18	— 19	— 16	— 12	— 6	— 2	0	3	2	3	4
— 7	— 12	— 14	— 15	— 14	— 12	— 6	— 2	0	3	3	5	5
— 6	— 9	— 11	— 13	— 13	— 11	— 5	— 2	1	3	4	5	5
— 4	— 7	— 7	— 11	— 12	— 10	— 5	— 2	1	3	4	5	5
— 3	— 5	— 6	— 9	— 9	— 7	— 3	— 2	0	3	3	5	5
— 1	— 2	— 3	— 6	— 8	— 6	— 3	— 1	0	2	3	5	5
25	10	— 5	— 20	— 30	— 35	— 30	— 23	— 15	— 6	— 9	— 12	— 15
4	— 15	— 32	— 45	— 50	— 55	— 55	— 50	— 37	— 28	— 18	— 15	— 13
— 11	— 32	— 50	— 64	— 70	— 75	— 75	— 62	— 40	— 23	— 10	— 5	— 6
— 22	— 45	— 63	— 80	— 88	— 93	— 85	— 66	— 30	— 7	8	8	0
— 30	— 55	— 72	— 88	— 95	— 95	— 85	— 62	— 20	— 2	10	10	3
— 37	— 64	— 78	— 95	— 97	— 92	— 76	— 50	— 13	12	10	10	4

	Φ	Local 12	13	14	15	16	17	18	19	20	21	22
Declination.	68	2	4	10	16	20	20	14	10	10	— 7	— 27
	67	4	5	12	18	17	17	10	7	3	— 11	— 31
	66	5	8	14	18	12	10	10	10	— 5	— 18	— 40
	65	7	11	15	14	8	6	10	5	— 10	— 23	— 44
	64	10	14	16	6	2	— 4	— 10	— 15	— 15	— 23	— 38
	63	2	4	6	5	0	— 4	— 13	— 20	— 25	— 27	— 27
	62	4	6	10	4	— 1	— 6	— 15	— 21	— 27	— 30	— 30
	61	6	8	8	4	— 3	— 6	— 19	— 25	— 30	— 31	— 27
	60	5	6	7	4	— 3	— 7	— 21	— 27	— 32	— 36	— 27
	59	5	6	7	4	— 3	— 7	— 23	— 28	— 33	— 30	— 27
	58	5	6	7	4	— 3	— 7	— 22	— 28	— 33	— 28	— 25
	57	0	4	4	2	— 3	— 7	— 18	— 24	— 25	— 23	— 21
	56	— 2	— 2	— 2	— 2	— 5	— 7	— 13	— 14	— 14	— 15	— 15
Hor. Intensity.	74	40	50	45	5	— 20	— 42	— 65	— 87	—100	— 80	— 63
	73	20	20	— 12	— 24	— 40	— 62	— 77	— 82	— 73	— 38	— 17
	72	55	40	25	10	— 25	— 55	— 80	— 90	— 90	— 80	— 60
	71	80	90	70	50	14	— 30	— 80	—125	—130	—120	—115
	70	75	80	80	70	42	10	— 65	—100	—120	—135	—150
	69	63	70	84	62	66	40	— 30	— 63	—100	—141	—190
	68	55	60	80	90	90	65	10	— 30	— 76	—122	—222
	67	43	50	75	95	95	80	45	0	— 53	—130	—220
	66	35	40	60	90	98	85	63	20	— 35	—110	—186
	65	26	32	40	75	92	75	70	43	— 15	— 91	—132
	64	15	18	26	50	70	80	70	55	10	— 65	—122
	63	2	6	10	20	30	40	40	20	4	— 40	— 65
	62	— 6	— 3	2	0	0	0	6	— 5	— 13	— 15	— 20
	61	— 11	— 11	— 11	— 4	— 4	— 4	— 5	— 10	— 14	— 12	— 13
	60	— 15	— 15	— 15	— 14	— 10	— 10	— 12	— 14	— 18	— 18	— 18
	59	— 16	— 16	— 16	— 14	— 14	— 14	— 18	— 20	— 20	— 20	— 20
	58	— 17	— 17	— 17	— 15	— 15	— 15	— 20	— 20	— 20	— 22	— 22
	57	— 18	— 18	— 18	— 17	— 17	— 17	— 20	— 20	— 20	— 22	— 20
	56	— 18	— 18	— 18	— 20	— 20	— 18	— 20	— 20	— 20	— 22	— 20
	55											
Ver. Intensity.	74	— 50	— 54	— 60	— 60	— 33	— 15	10	31	51	75	93
	73	— 37	— 48	— 53	— 48	— 41	— 22	5	30	52	72	101
	72	— 28	— 44	— 55	— 67	— 70	— 60	— 40	— 7	28	60	104
	71	— 20	— 39	— 58	— 82	— 83	— 82	— 77	— 58	— 27	44	102
	70	— 8	— 30	— 55	— 71	— 79	— 72	— 80	— 73	— 60	25	90
	69	2	— 14	— 32	— 55	— 68	— 60	— 77	— 77	— 66	7	72
	68	13	5	— 15	— 22	— 40	— 48	— 72	— 76	— 66	— 10	52
	67	22	28	22	— 8	— 10	— 36	— 62	— 66	— 60	— 29	26
	66	27	32	24	18	2	— 15	— 32	— 50	— 51	— 47	— 20
	65	30	35	35	30	22	3	— 18	— 40	— 46	— 62	— 53
	64	31	42	47	52	46	33	10	— 22	— 40	— 66	— 95
	63	22	30	36	50	53	52	53	25	— 4	— 42	— 62
	62	16	19	27	37	47	56	58	48	23	— 2	— 30
	61	14	18	24	32	42	52	56	47	24	2	— 22
	60	14	17	21	28	39	48	51	43	24	4	— 17
	59	14	17	18	24	33	43	46	38	22	4	— 13
	58	14	17	17	22	31	37	40	33	20	4	— 12
	57	12	13	13	20	26	33	35	29	18	5	— 8
	56	8	7	8	17	22	28	29	24	16	6	— 5
	55	6	6	6	13	17	22	22	19	13	5	— 3
	54	2	4	4	11	12	16	16	11	8	4	0
	53	0	3	2	9	8	10	10	8	7		

time												
23	24	1	2	3	4	5	6	7	8	9	10	11
— 45	— 71	— 85	—100	— 98	— 86	— 62	— 35	— 5	5	10	10	5
— 53	— 78	— 90	—103	— 97	— 80	— 43	— 17	4	10	12	10	5
— 60	— 87	— 92	—102	— 90	— 62	— 23	— 2	9	14	13	10	6
— 63	— 93	— 93	— 90	— 65	— 35	— 12	5	11	13	12	9	9
— 50	— 50	— 50	— 40	— 30	— 12	— 3	5	8	10	10	6	5
— 27	— 30	— 30	— 27	— 16	— 8	— 3	3	5	6	9	6	5
— 30	— 24	— 24	— 21	— 13	— 7	— 4	3	5	5	6	6	5
— 25	— 22	— 20	— 17	— 11	— 7	— 4	2	4	4	6	6	6
— 25	— 20	— 20	— 14	— 8	— 5	— 3	2	4	4	5	5	5
— 23	— 18	— 18	— 13	— 7	— 4	— 2	2	3	3	5	4	3
— 21	— 17	— 16	— 11	— 6	— 2	0	3	5	5	4	4	3
— 18	— 15	— 13	— 10	— 6	— 4	— 2	0	0	0	— 1	2	2
— 15	— 14	— 10	— 9	— 5	— 5	— 5	— 3	— 3	— 3	— 3	— 3	— 3
— 60	— 66	— 70	— 90	—100	—104	—104	—108	— 74	— 40	— 8	16	35
— 20	— 33	— 38	— 36	— 30	— 30	— 40	— 60	— 40	— 18	28	26	46
— 40	— 80	—100	—116	—100	—100	—105	— 63	— 42	— 14	15	37	60
—122	—160	—165	—170	—170	—170	—140	—100	— 55	— 14	22	45	70
—200	—215	—215	—215	—195	—185	—140	—105	— 52	— 12	24	44	70
—260	—262	—262	—244	—215	—194	—135	— 90	— 40	— 10	22	40	64
—295	—300	—300	—270	—235	—195	—125	— 72	— 28	— 8	16	29	50
—295	—320	—320	—290	—242	—185	—110	— 57	— 18	— 2	10	20	35
—270	—325	—325	—295	—222	—160	—100	— 45	— 17	— 2	5	15	25
—230	—305	—330	—295	—188	—128	— 85	— 35	— 13	— 5	0	10	18
—185	—240	—240	—200	—150	—100	— 65	— 35	— 20	— 10	— 6	0	3
—100	—120	—120	—110	— 70	— 50	— 35	— 30	— 18	— 16	— 10	— 10	— 7
— 30	— 40	— 40	— 40	— 30	— 20	— 10	— 20	— 12	— 12	— 10	— 10	— 10
— 17	— 30	— 30	— 30	— 15	— 8	— 2	— 16	— 10	— 10	— 6	— 6	— 6
— 18	— 18	— 18	— 18	— 18	— 18	— 18	— 18	— 18	— 18	— 18	— 18	— 18
— 20	— 25	— 25	— 20	— 20	— 20	— 20	— 20	— 20	— 20	— 20	— 20	— 20
— 25	— 20	— 20	— 15	— 18	— 18	— 18	— 18	— 18	— 18	— 18	— 18	— 18
— 25	— 16	— 16	— 14	— 15	— 15	— 14	— 15	— 15	— 15	— 15	— 15	— 15
— 15	— 12	— 12	— 12	— 12	— 12	— 12	— 12	— 12	— 12	— 12	— 12	— 12
	— 10	— 10	— 10	— 10	— 10	— 10	— 10	— 10	— 10	— 10	— 10	— 10
106	115	125	126	108	97	70	50	30	5	— 15	— 20	— 42
122	140	147	144	130	115	79	52	38	7	— 6	— 15	— 23
134	157	162	157	146	122	78	34	12	— 8	— 11	— 9	— 12
140	166	170	163	154	124	71	10	— 15	— 22	— 16	— 4	— 4
143	161	150	135	115	100	42	— 19	— 30	— 25	— 18	2	4
112	130	110	85	70	35	4	— 41	— 39	— 25	— 17	7	12
82	89	70	45	12	— 30	— 46	— 58	— 44	— 25	— 13	9	17
45	45	35	15	— 40	— 73	— 80	— 68	— 47	— 23	— 8	10	20
17	25	19	0	— 17	— 40	— 60	— 60	— 38	— 18	— 6	9	21
— 10	12	10	— 17	— 65	— 65	— 56	— 45	— 29	— 15	— 4	8	21
—112	—133	—135	—132	—103	— 85	— 73	— 46	— 27	— 13	— 2	10	10
— 90	—100	—110	—110	— 85	— 70	— 58	— 42	— 23	— 12	0	7	16
— 55	— 75	— 85	— 85	— 72	— 68	— 44	— 32	— 19	— 10	0	7	13
— 45	— 63	— 72	— 72	— 65	— 54	— 38	— 27	— 17	— 8	0	6	11
— 37	— 54	— 62	— 62	— 55	— 45	— 34	— 24	— 14	— 6	0	6	10
— 31	— 46	— 53	— 53	— 47	— 38	— 28	— 21	— 12	— 4	1	6	10
— 25	— 36	— 42	— 42	— 38	— 32	— 24	— 17	— 10	— 3	0	6	9
— 18	— 23	— 29	— 29	— 30	— 26	— 19	— 14	— 8	— 3	0	5	8
— 13	— 17	— 22	— 23	— 25	— 21	— 17	— 11	— 7	— 2	0	4	7
— 9	— 13	— 17	— 17	— 17	— 15	— 12	— 8	— 4	— 2	0	4	5
— 4	— 9	— 12	— 12	— 12	— 9	— 7	— 5	— 3	— 2	0	4	4
	— 6	— 9	— 9	— 7	— 6	— 5	— 3	— 3	— 2	0	3	3

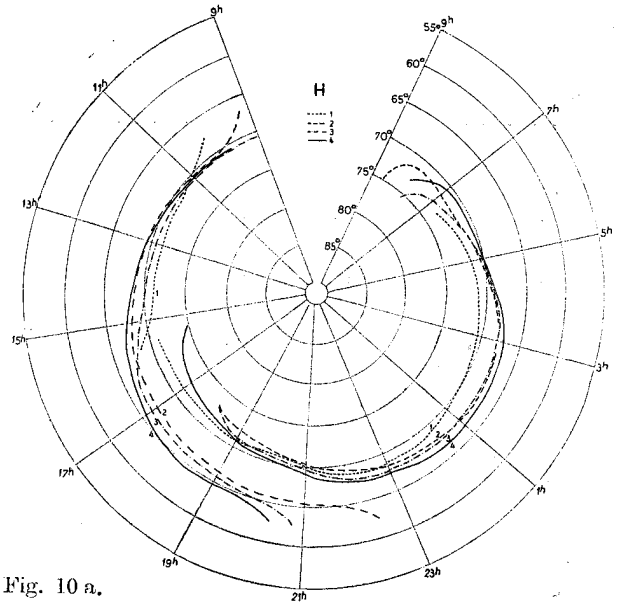

Fig. 10 a.

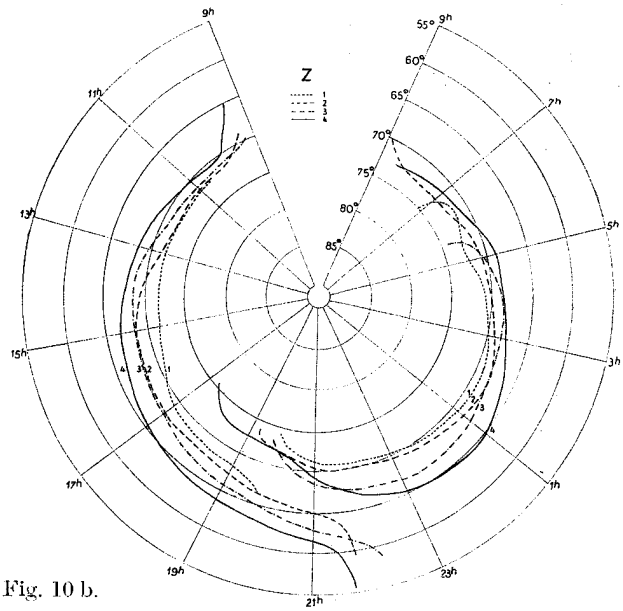

Fig. 10 b.

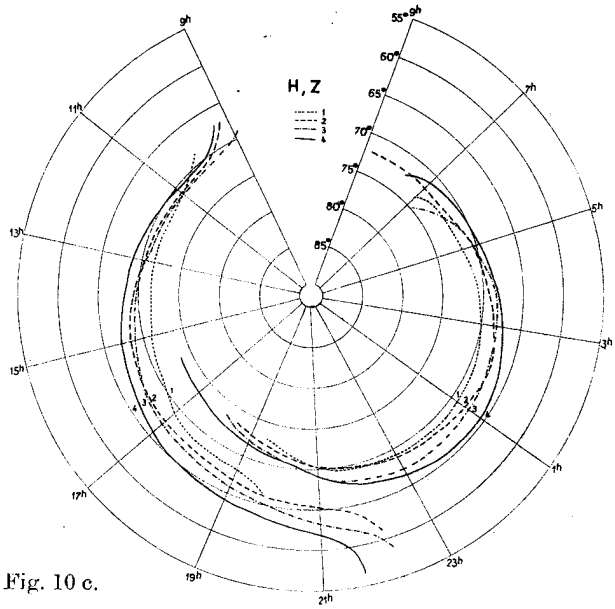

Fig. 10 c.

Fig. 10 a, b and c. Position of the „auroral zones" for different ranges of storminess. a and b from the $\triangle H$- and $\triangle Z$-fields, c represents the mean position from both fields.

tain evidence which supports this point of view. In their analysis of the mean daily disturbance vector, Vestine[1] and Vestine and Chapman[2] used the material from a number of stations lying along the whole auroral zone around the globe. In spite of the great differences in longitudes of the different stations, all values fitted together on a smooth curve when going from north to south across the auroral zone. For the positive maximum in the afternoon and the negative maximum of disturbance at midnight, there are thus no longitude effects along the auroral zone. For a closer examination, especially of the discontinuities of the auroral zone and the „positive" and „negative" sections, the material is not sufficient. In order to solve this question one ought to have a similar dense net of recording stations along a meridian lying on the American side of the polar region, say along the 260° geomagnetic longitude, as along the line from Spitzbergen over Bear Island and the Scandinavian peninsula.

3. THE HEIGHT AND DIMENSIONS OF THE DISTURBING CURRENT SYSTEMS

In his analysis of the vectors along the auroral zone and the D-field, Birkeland for the first time, obtained an estimate of the disturbing current systems height and current intensity. Assuming that the perturbing current system can be regarded as a narrow cylindrical current, it is possible to calculate the dimensions of this current system from the perturbing vectors recorded at two stations lying at suitable distances. Birkeland[3] analyzed a number of cases and got heights above the earth's surface of the current system lying between 160 and up to 1000 km. The greater part of height determinations gave values lying in the range 300—600 km. The total current intensity was of the order 600 000—1 000 000 amps.

As for the quiet diurnal variation of the earth's magnetic field one must, however, assume that in the deflections recorded during magnetic storms a certain fraction also is due to the field

[1] Vestine, Terr. Mag. *43*, 261 (1938.
[2] Vestine and Chapman, Terr. Mag. *43*, 351 (1938).
[3] Loc. cit: p. 307—310.

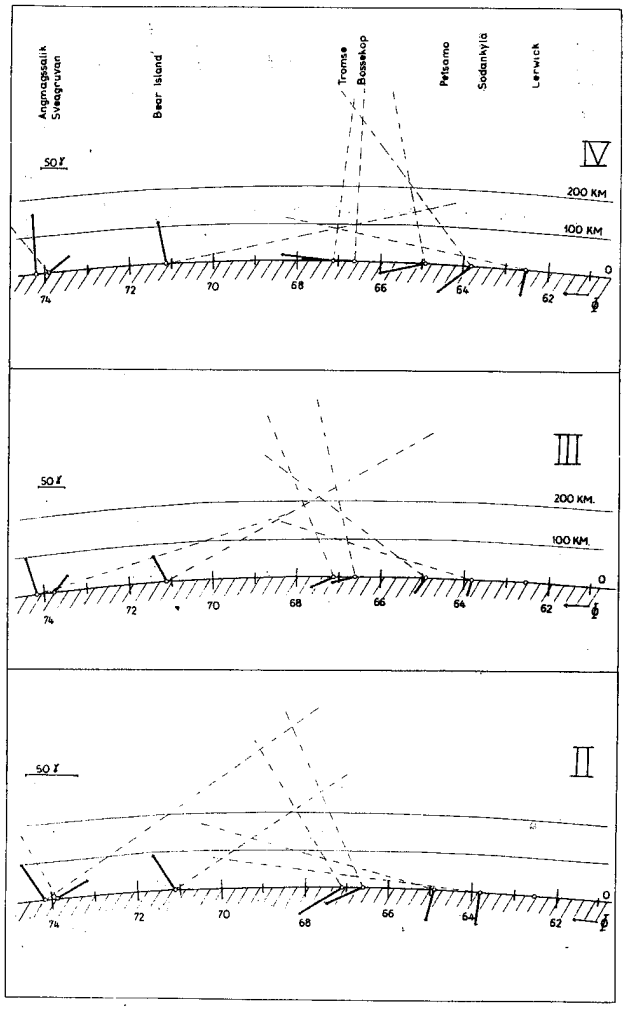

Fig. 11 a. Perturbing vectors in a vertical plane lying in the geomagnetic meridian. Afternoon-disturbance at about 17^h local time.

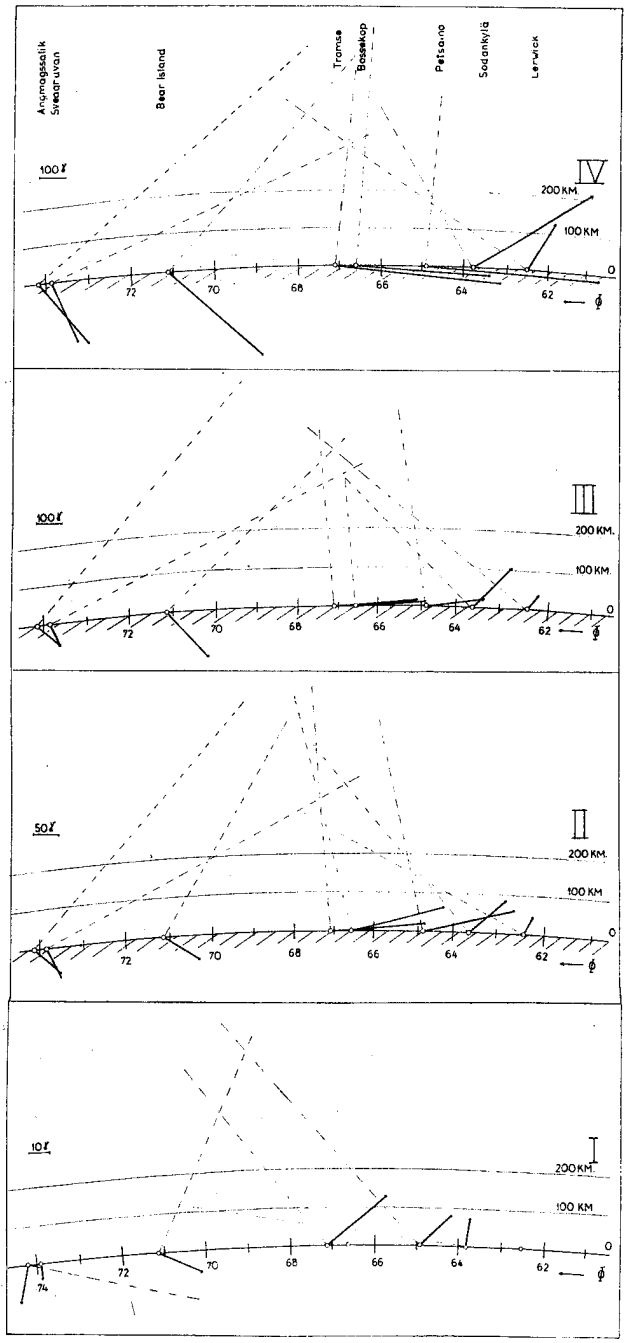

Fig. 11 b. Perturbing vectors in a vertical plane lying in the geomagnetic meridian. Midnight-disturbance at about 24^h local time.

of the earth currents. The D-field recorded therefore constitutes two parts, the external part D_e due to the perturbing current system overhead, and an internal part, D_i due to the field of the induced earth currents. Chapman[1] has pointed out that it is likely to assume that in H the internal and external parts of the disturbing vector will be similar in direction, whereas in Z the two components will have opposite signs. We thus, when using the perturbing vector without reduction for the influence of the earth currents, overestimate the component in H and underestimate the component in Z. When the effect of the earth currents are taken into consideration, the consequence will be to *lower* the height of the perturbing current system calculated according to Birkeland's method. Concerning the fraction of the disturbing vector which arises from the external current system, a magnitude of 0.6 is likely to be assumed, the same value which comes out in the analysis of the quiet diurnal variation. Chap-

[1] Terr. Mag. *40*, 349 (1935).

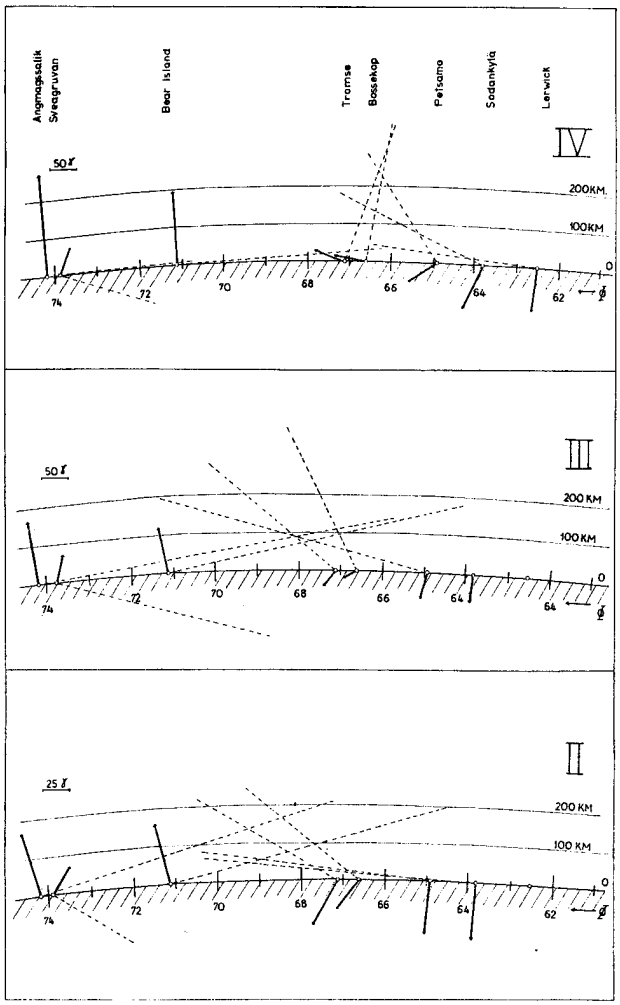

Fig. 12 a. Perturbing vectors in a vertical plane lying in the geomagnetic meridian. Afternoon-disturbance at about 17^h local time. The perturbing vectors have been reduced for the effect of the assumed earth currents.

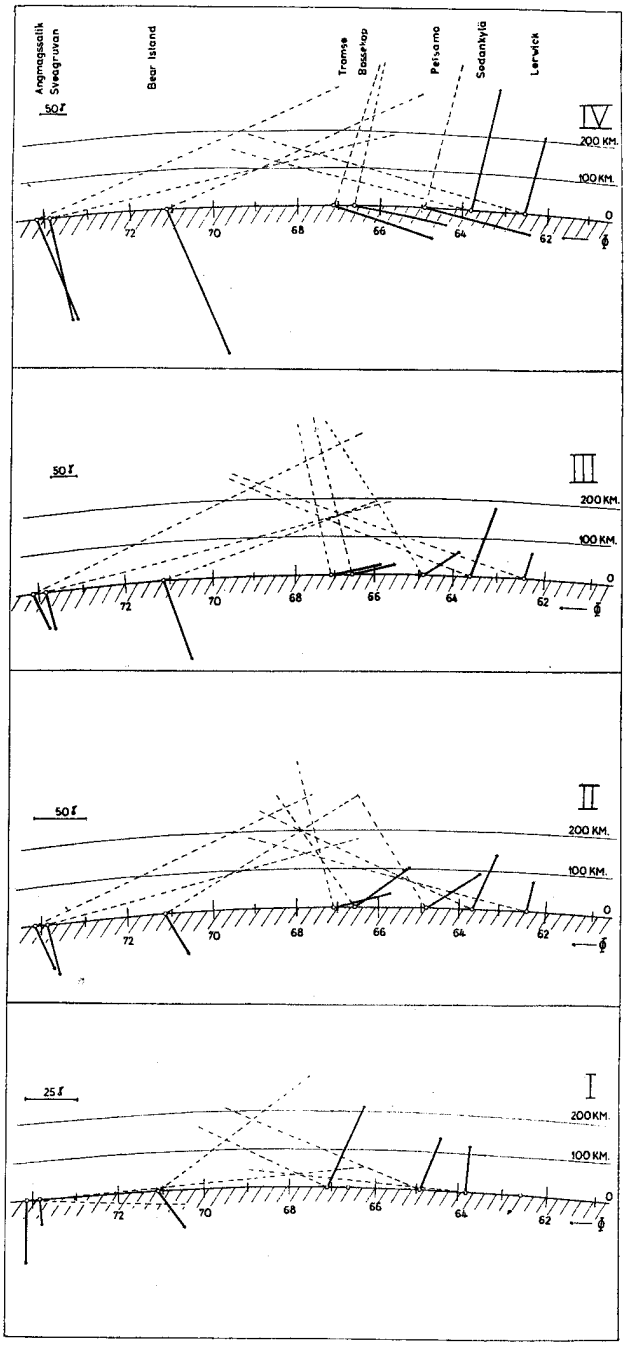

Fig. 12 b. Perturbing vectors in a vertical plane lying in the geomagnetic meridian. Midnight-disturbance at about 24^h local time. The perturbing vectors have been reduced for the effect of the assumed earth currents.

man[1] and McNish[2] have used this value in their analysis of the *D*-field.

In fig. 11 a and b and fig. 12 a and b the positions of the mean disturbance vectors for a number of observatories during the maximum phase in the afternoon and at midnight have been drawn up in a vertical plane lying in the geomagnetic meridian. The curvature of the earth is taken into consideration, and the direction from each observatory to the perturbing current system is marked off with broken lines. In fig. 11 a and b the perturbing vectors actually recorded are drawn up; in fig. 12 a and b the effect of the earth currents has been taken into consideration in the *H* and *Z* directions.

In fig. 11 and 12 the directions to the perturbing current all converge against a certain range of heights. Concerning the accuracy we must regard the perturbing vectors during the

[1] Vestine and Chapman, Terr. Mag. *43*, 351 (1938).
[2] McNish, Terr. Mag. *43*, 67 (1938).

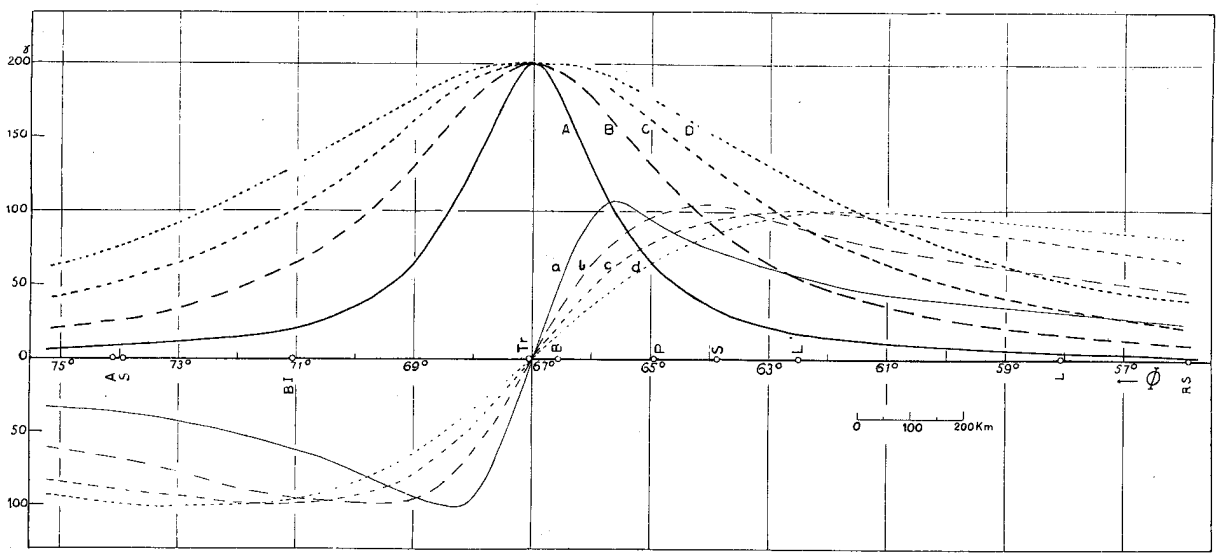

Fig. 13. Variation of $\triangle H$ and $\triangle Z$ with geomagnetic latitude Φ due to a linear and infinite current perpendicular to geomagnetic meridian at $\Phi = 67°$. A, B, C and D give the variation in $\triangle H$ due to a current lying at heights of 150, 300, 450 and 600 km respectively with current strengths of 1.5, 3.0, 4.5 and $6.0 \cdot 10^6$ amps. respectively. a, b, c and d show the variation in $\triangle Z$ for the same current values.

midnight phase, fig. 11 b and 12 b, to be considerably more reliable than the smaller vectors during the afternoon phase, and in the discussion of numerical values we therefore exclude the determinations from the afternoon phase. From fig. 11 b it is evident that the directions to the perturbing current system converge towards a point or area lying at an height of 300—400 km, which is the same range of heights deduced by Birkeland in his memoir. When the perturbing vectors are being reduced for the effects of the induced earth currents, as in fig. 12 b, the heights of the perturbing current system are considerably lowered, and the directions converge towards a point lying at height of about 150 km or slightly above this. McNish[1] in his careful analysis of one single case of a negative polar storm lying above Tromsø, comes to the conclusion that the equivalent line-current is located at a height not greater than 200 km. In his analysis he has considered the effect of the induced earth currents.

A comparison between the figures 11 b and 12 b reveals, however, a serious discrepancy concerning the variation of the perturbing vectors with Φ, in the case when the perturbing vectors have been reduced for the effect of the assumed induced earth currents. On fig. 12 b we see that in this case the perturbing vectors at Tromsø and Bossekop, these stations lying underneath the perturbing current system, are less than the pertubing vectors recorded at Bear Island and Sodankylä. The strong reduction of the perturbing vectors at Tromsø and Bossekop from fig. 11 b to 12 b is due to the fact that for Tromsø and Bossekop the vectors are almost horizontal and the assumed effect of the earth currents has to be subtracted from the observed values. At Bear Island and Sodankylä, however, there is a considerable vertical component of the perturbing vector, and the assumed effect of the earth currents for these stations are to be added to the component. Without any calculations it is evident that with an assumed effect of the earth currents where the external part of the perturbing vector is only 0.6 of the recorded value, this leads to serious discrepancies regarding the variation of the perturbing vector with Φ.

It is worth while to consider these discrepancies in detail. The variation of the perturbing forces in H and Z with Φ have therefore been calculated for certain values of perturbing currents, these lying in *different heights*. Fig. 13 shows graphically the variation of $\triangle H$ and $\triangle Z$, both lying in the geomagnetic meridian. The current is assumed to be linear and infinite moving perpendicular to the geomagnetic meridian at

[1] McNish, Terr. Mag. *43*, 67 (1938).

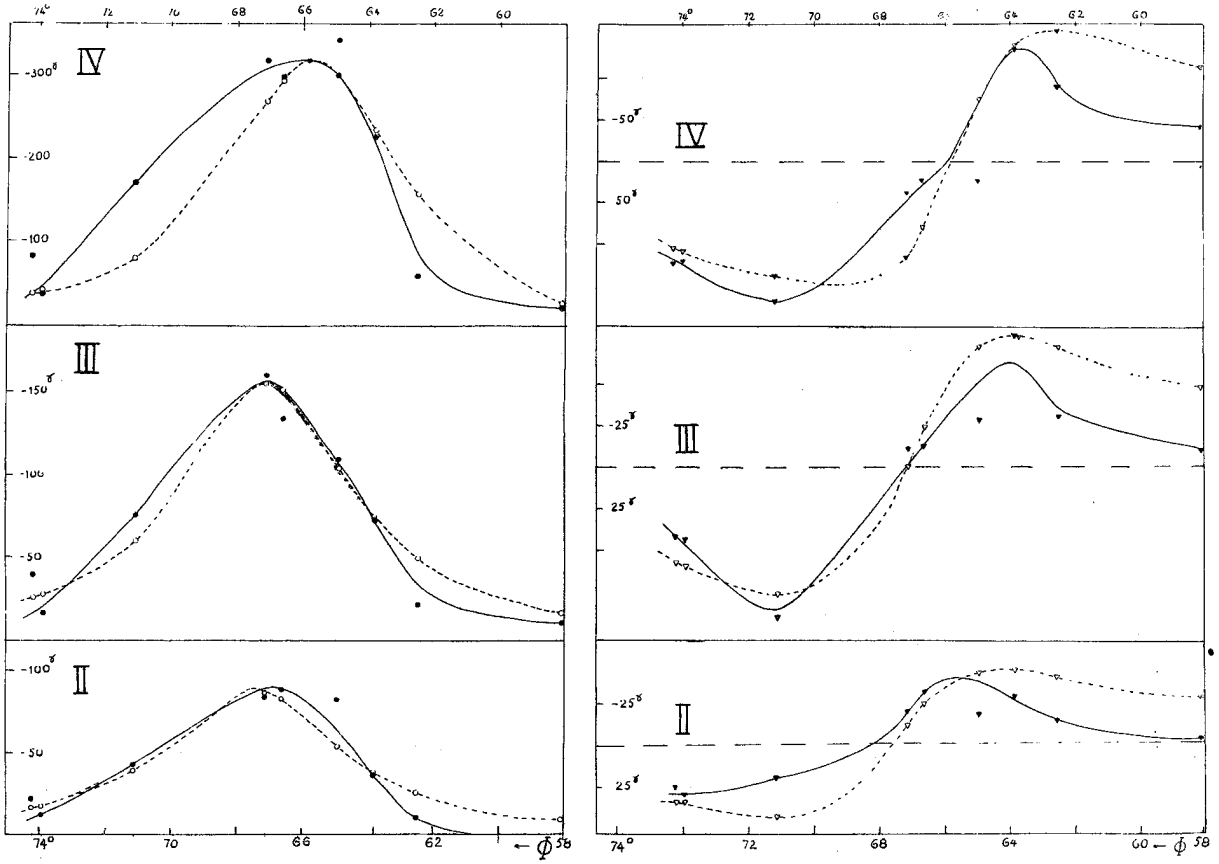

Fig. 14. ●——▼ observed values of $\triangle H$ and $\triangle Z$,
○——▽ calculated » » $\triangle H$ » $\triangle Z$ due to a linear current in 350 km height.
Maximum phase at midnight for ranges IV, II and II.
(Each point indicate the position of a recording station.)

$\Phi = 67°$. In all four cases the perturbing force on the earth's surface just underneath the current is assumed to be 200 gammas, and is thus horizontal. The heights of the perturbing current systems are assumed to be 150, 300, 450 and 600 km. Under these assumptions the current strengths will be respectively 1.5, 3.0, 4.5 and $6.0 \cdot 10^6$ amps. The calculations have been made for a plane earth.

In order to get a close comparison between the observed variation in $\triangle H$ and $\triangle Z$ and the values calculated from the current model, the observed and calculated values for the midnight maximum phase for ranges IV, III and II are shown in fig. 14 and 15. In fig. 14 the observed values of $\triangle H$ and $\triangle Z$ have been used without reduction for the assumed effect of earth currents. The perturbing current is laid at a height of 350 km which fig. 11 a and b indicate, and the current strengths in each of the three cases are calculated from the observed values of $\triangle H$ just below the current.

In fig. 15 the values of $\triangle H$ and $\triangle Z$ observed have been reduced for the assumed effect of the earth currents, and the height of the perturbing current is laid at 160 km, which was indicated by fig. 12 a and b. The current strengths were calculated from the value of $\triangle H$ just below the current.

Table 6.

	No effect of earth current assumed. Perturbing current height 350 km		$\triangle H$ and $\triangle Z$ have been reduced for the effect of assumed earth currents. Perturbing current height 160 km	
Range	$\triangle H$ max	Current strength	$\triangle H$ max	Current strength
	gammas	10^6 amps.	gammas	10^6 amps.
IV	320	5.6	200	1.6
III	155	2.7	96	0.8
II	88	1.5	53	0.4

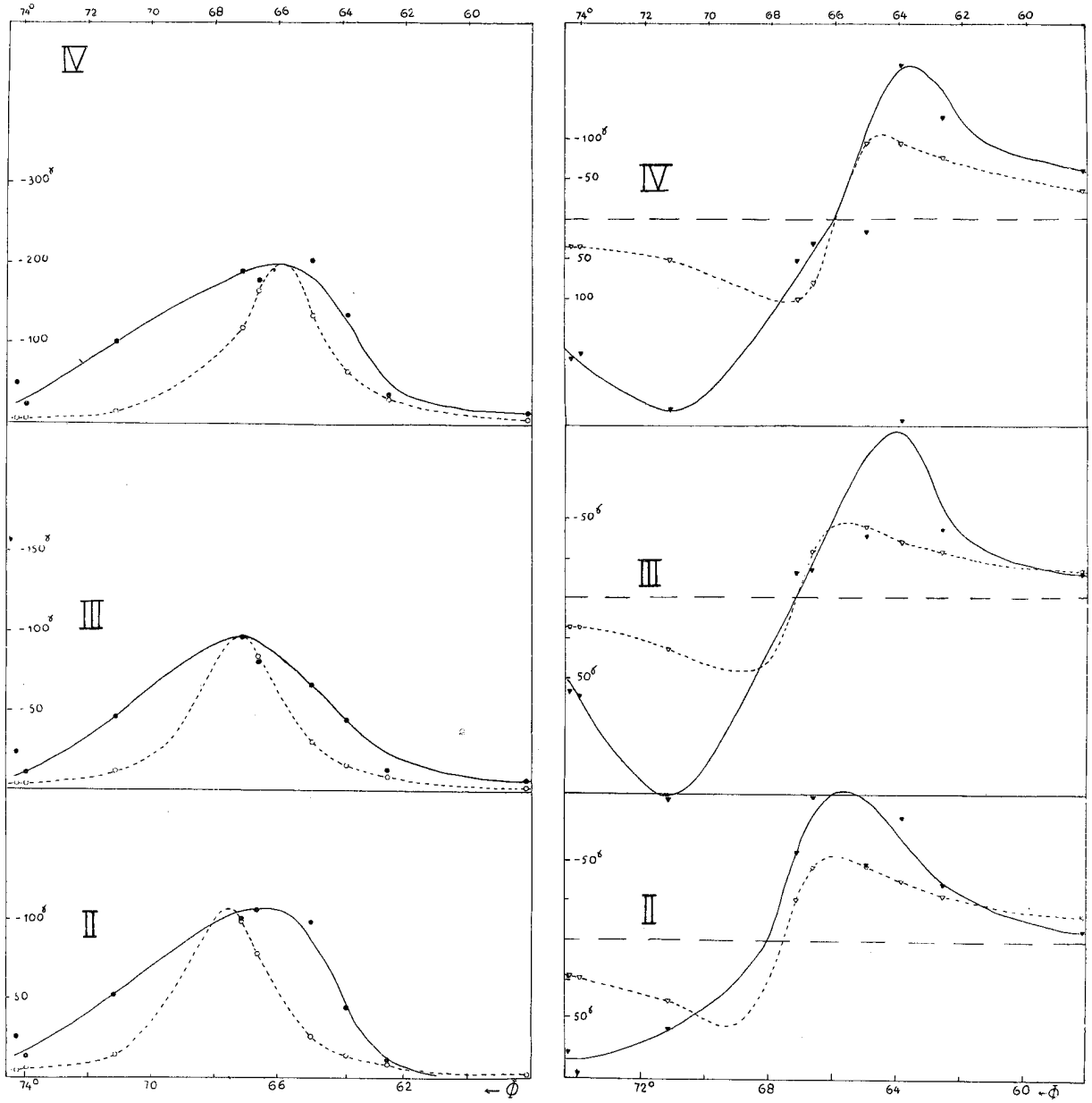

Fig. 15. ▼——● observed values of $\triangle H$ and $\triangle Z$, the values being reduced for the effect of the assumed earth currents,
▽——○ calculated values of $\triangle H$ and $\triangle Z$ due to a linear current lying in 160 km height. Maximum phase at midnight for ranges IV, III and II.
(Each point indicate the position of a recording station.)

In table 6 are the heights and strengths of the perturbing currents for the two alternatives given.

Although there is a considerable scattering of the observed values in fig. 14 and 15, there seems to be no doubt about the general shape of the mean curve. In fig. 14, where the model current is in 350 km height, there is a fairly good agreement between the mean curve observed and the calculated values from the model current. Common for all ranges, is the more rapid decrease of $\triangle H$ observed with decreasing values of Φ, when compared with the calculated values. For $\triangle Z$ there is also a parallel variation in the observed and calculated values, but also here the observed values decrease rapidly with decreasing values

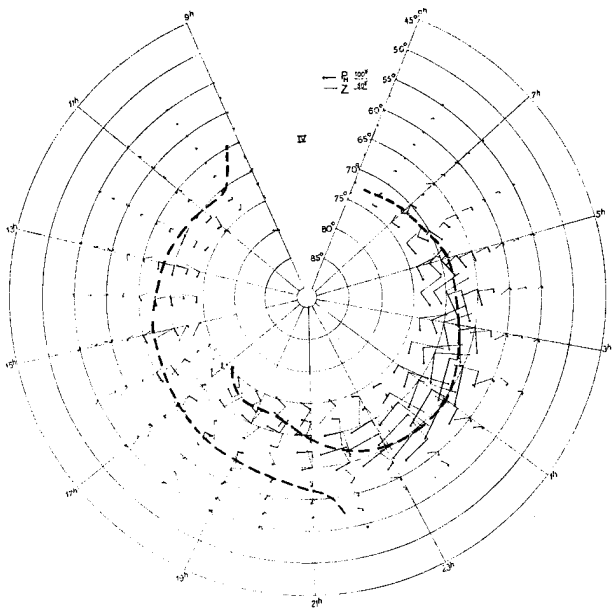

Fig. 16. Current-arrows indicating directions and strengths of hypothetical overhead currents. Diurnal variation of the currents across a geomagnetic meridian at about $\Lambda = 120$ °.

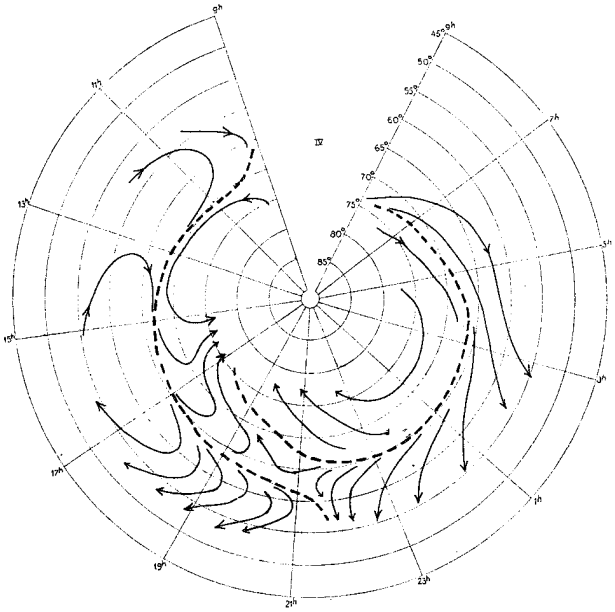

Fig. 17. Mean direction of in- and outflow of currents, determined from the position of the current-arrows in fig. 16.

of Φ when compared with the values calculated.

In fig. 15, where the observed values have been reduced for the effect of the assumed earth currents, the agreement between the values observed and the values calculated, is by far so good as in the first alternative. In this last case the current height is only 160 km, and the H curve thus gets a steep maximum which does not appear in any of the three curves observed. In $\triangle Z$ the discrepancies are even greater. Here the observed values lie far over the values calculated. It is evident that the observed variation in $\triangle Z$, which shows maximum values even greater than the maximum values in $\triangle H$, are impossible to explain for current systems lying at *any* height chosen. According to fig. 13 the maximum value of $\triangle Z$ will always be considerably smaller than the maximum value of $\triangle H$ for any height chosen of the current system.

From fig. 14 and 15 we may draw the conclusion, that if the observed values of $\triangle H$ and $\triangle Z$ are being reduced for the effect of the assumed earth currents, this leads to a variation in $\triangle Z$ *which cannot be accounted for by a current system lying in any height.*

If, however, the earth current effect is *reduced* from 0.4 to about 0.1 of the entire field, we will get an even better agreement between the observed values and calculated values for $\triangle Z$, than shown in fig. 14. It is, however, doubtful whether there is any sense in extending the numerical calculations in order to get a closer agreement. The underlying assumption of a linear and infinite current system, which should be responsible for the perturbations, is in itself an hypothesis which must not be regarded as corresponding too strictly with the conditions really occurring. In fact, the problem to compute the dimensions of a current system from the perturbing forces observed on the earth's surface, is mathematically indeterminable, and it must be regarded as surprising that so many details of the observed variations can be explained by the rough hypothesis of a linear current system.

Birkeland regarded the currents calculated from earth-magnetic perturbations as real free currents, probably consisting of free electrons, coming in from the space towards the auroral zone and bent back again. He investigated the effects of various models, and especially favoured a model consisting of a descending and ascending branch connected with a segment parallel with the auroral zone. After the time of Birkeland,

the existance of such free electron currents has been doubted. During the last decades, the problems of the quiet diurnal variation have been worked through theoretically, and according to the dynamo theory the quiet diurnal variation is explained by the movement of the ionized air in heights of or just above the *E*-layer, across the permanent earth magnetic field. During earth-magnetic storms we know from radio echo experiments that the electron density. and, simultaneously, the conductivity, is raised considerably, and according to modern views it has been assumed that the magnetic storms may be explained by a similar process as the quiet diurnal variation. This means that the currents deduced from the perturbing vectors must lie at the same heights as the upper part of the *E*-layer, 120—150 km. Further, as the currents are now assumed to flow in the *E*-layer, they must be *closed* and it should be possible to construct current charts from the perturbing vectors for the storms in the same manner as has been done for the quiet diurnal variation.

In order to investigate this point more closely, it will be convenient to use Birkeland's mode of representing the perturbing vectors as „current-arrows". In this case a horizontal current-arrow is drawn at right angles to the horizontal perturbing vector, P_H, and of equal length. The vertical component of the perturbing force is indicated by another line at right angles. In fig. 16 the current-arrows at each intersection between geomagnetic longitude and latitude is drawn up for the case of range IV, using the values in table 4.

From fig. 16 we get an impression of the main directions of the two current sytems appearing, positive or eastwards directed, at about 17^h in the afternoon and the negative or westwards directed at midnight. We also see that north of the auroral zone there is a distinct inflow of currents from the polar cap. South of the auroral zone on lower latitudes there is a gradual outflow of currents, and during the afternoon maximum the small perturbing currents at lower latitudes of $\Phi \sim 55°$ are directed opposite. We thus get an impression of a tendency to form closed current systems. In fig. 17 the main directions of the in- and outflow of currents have been indicated.

We must, however, point out that only a small fraction of the entire current system along

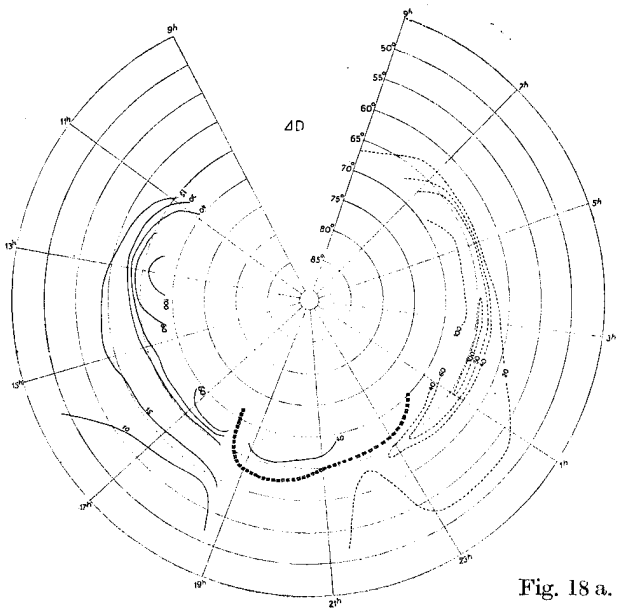

Fig. 18 a.

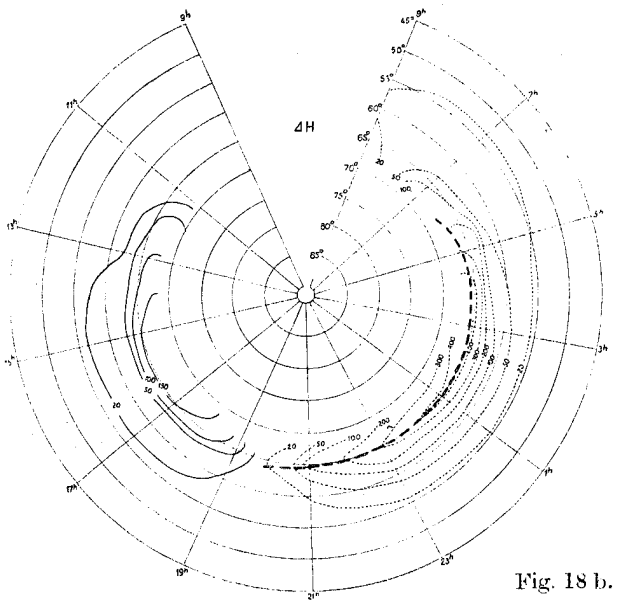

Fig. 18 b.

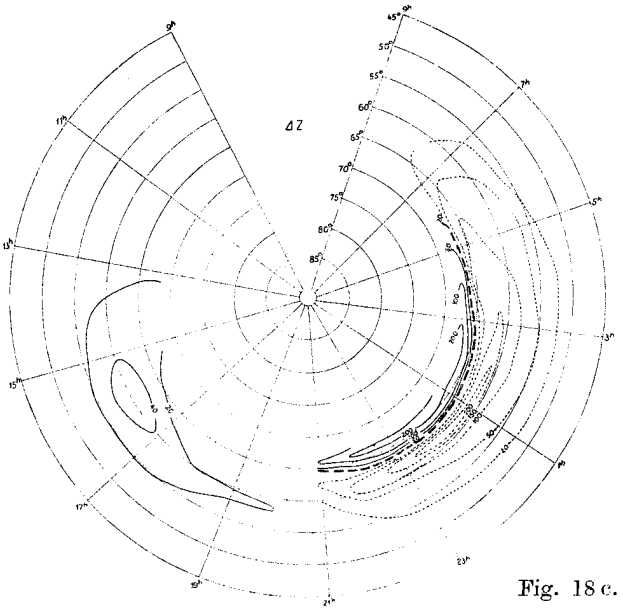

Fig. 18 c.

Fig. 18 a, b and c. Variation of the three components ($\triangle D$, $\triangle H$ and $\triangle Z$) of the *D*-field with local time across the 120° geomagnetic meridian. Mean values of the nine greatest storms in the period 1932—37.

the auroral zone seems to be divided out and run back as a „rückstrom" on lower latitudes. Quantitatively we see this from the small values of the current arrows of reversed direction on lower latitudes. Further, would a „rückstrom" of considerable strength completely alter the direction of $\triangle Z$. If a substantial „rückstrom" existed, this would mean that in the centre of this ring, current one would have a maximum in $\triangle Z$. This is by no means the fact.

From the discussion above we must conclude that although there seems to exist a „rückstrom" effect on lower latitudes, the strength of this current is small, and it is not possible from this to conclude that the hypothetical perturbing currents flowing in the ionosphere are closed. As to the „rückstrom" effect over the polar cap, the fig. 16 and 17 indicate that also here a „rückstrom" exists. The material is, however, not sufficient to support the view that the perturbing currents as *a whole* are closed over the polar cap.

4. THE FIELD OF DISTURBANCE OF THE GREATEST STORMS

In the previous chapters the material used in the discussion of the *D*-field was selected from the Polar-Year 1932—33 records, which was a year of minimum activity with very few storms of the very greatest range. On the other hand, the net of recording stations was more extended than ever before, having stations at our disposal which were conveniently distributed north of the auroral zone. It would be of interest to investigate to what extent the *normal* and permanent distribution of observatories on the Scandinavian peninsula and southwards would be able to give a description of the more important features of the *D*-field and the position of the auroral zone during storms. It is evident from the previous discussion that this will only be the case during very intense storms when the auroral zone is being well displaced towards south, Tromsø thus lying in the *northern* part of the *D*-field.

Table 7.

Day	*C*
August 27—28, 1932	1.9
June 7— 8, 1935	1.7
July 10—11, 1936	1.5
May 27—28, 1937	1.7
» 28—29, »	1.5
June 5— 6, »	1.6
July 6— 7,	1,2
» 9—10, »	1.2
» 23—24, »	1.5
Mean	1.53

From the Tromsø year-books the nine most intense storms were selected for the period 1932 — 37, all having daily sums of absolute storminess (AS) greater than 4000 gammas. The days selected are given in table 7, C is the mean international character number of the day. The mean diurnal variation of storminess in D, H and Z according to local time for a number of observatories, is given in table 8. In fig 18 a, b and c the diurnal variation of the *D*-field over Scandinavia across a geomagnetic meridian at about $\Lambda = 120°$ is shown in the same way as in the fig. 6—9.

A comparison between fig. 18 and the corresponding fig. 9, the latter demonstrating the *D*-field for range IV, shows no fundamental differences. There is an increase in the maximum values of $\triangle H$ and $\triangle Z$ and a corresponding slight displacement of the auroral zone towards south. For the greatest storms the value of the geomagnetic latitude of the auroral zone during the maximum phase at 24^h is about $\Phi = 64°$. For the maximum positive phase at about 16^h, however, the net of recording stations has not been sufficient for drawing up the complete set of curves on the maps.

In order to get a complete picture of even the main features of the *D*-field we must therefore regard the distribution of the permanent recording stations as being insufficient. It is of special importance to have one or two stations lying closely north of the auroral zone. Bear Island and a station at the southern part of Spitzbergen seems to be the most convenient places. In order to get a complete picture of the *D*-field it is of far greater importance to have two such stations permanently in operation, than to erect or maintain permanent recording stations on lower latitudes.

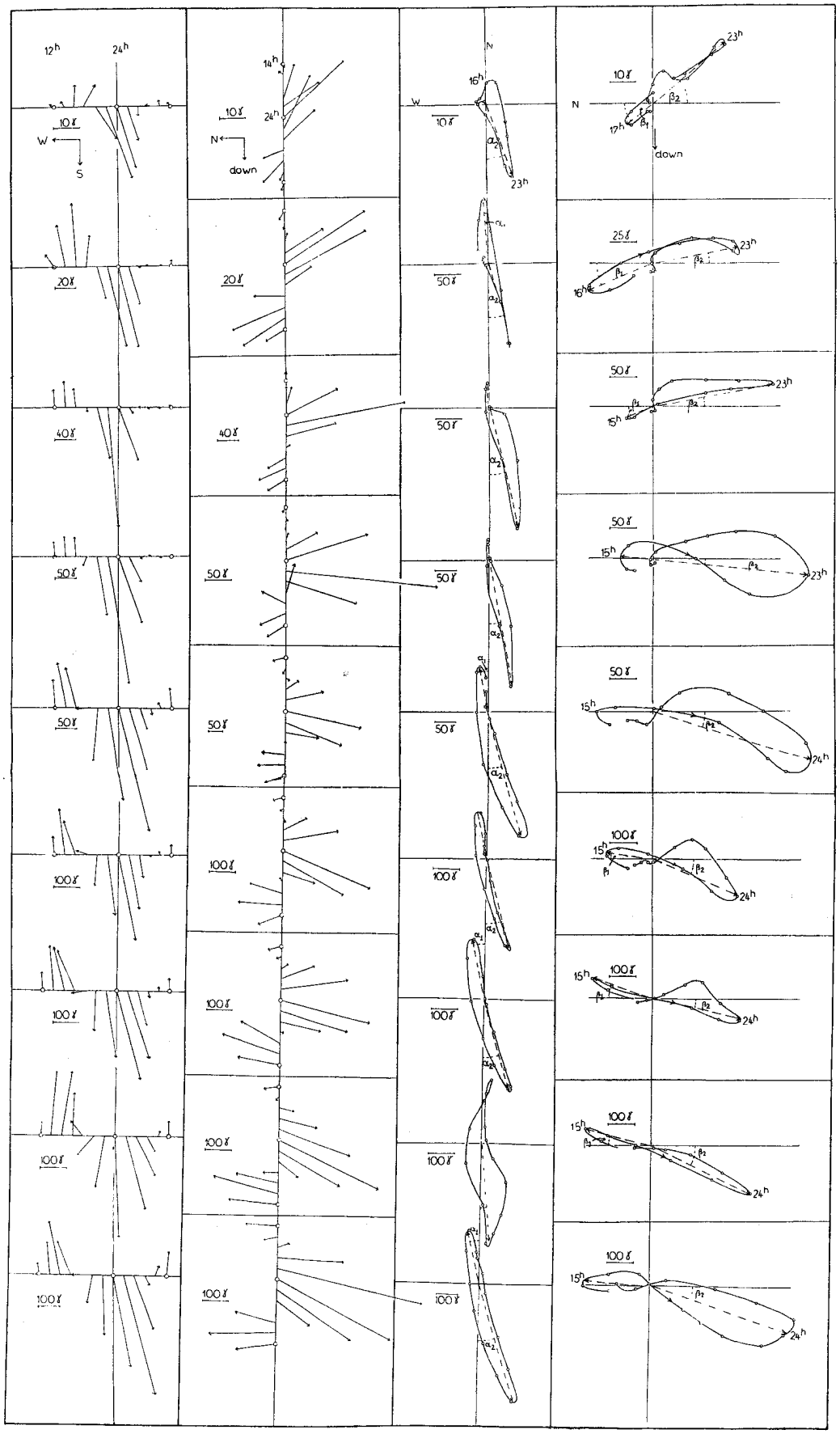

Fig. 19. Vector diagrams in horizontal and vertical planes for nine different ranges of disturbance from Tromsø for the period 1930—44.

Table 8. Mean diurnal variation of Storminess (S_D) in gammas at different observa-

		Local												
		11	12	13	14	15	16	17	18	19	20	21	22	23	24
Declination.	Tromsø	8	8	10	20	46	50	60	65	60	50	40	28	15	—10
	Abisko	13	22	30	37	44	50	56	60	60	50	27	16	— 8	—55
	Sodankylä ..	— 5	— 5	— 8	—20	—30	—40	—46	—44	—35	—27	—23	—35	—50	—85
	Lerwick	2	3	6	7	9	10	11	11	10	5	0	—10	—22	—32
	Lovø	6	6	7	10	14	17	15	9	2	— 5	—11	—18	—25	—28
	Rude Skov .	10	12	14	16	17	15	8	1	— 5	—10	—15	—22	—27	—27
	Potsdam ...	5	7	9	11	11	10	9	5	0	— 5	—10	—15	—20	—24
Hor. Intensity.	Tromsø	18	60	100	150	200	232	212	145	55	—15	— 85	—150	—250	—320
	Abisko	22	60	90	135	175	190	165	120	60	—20	—120	—210	—277	—353
	Sodankylä ..	20	45	72	82	115	150	165	130	70	—25	—100	—180	—255	—400
	Lerwick	10	14	19	23	28	36	42	44	37	2	— 52	— 92	—122	—148
	Lovø	6	9	13	18	26	32	34	32	25	10	— 9	— 26	— 39	— 44
	Rude Skov .	5	6	9	12	15	15	12	7	— 3	—13	— 19	— 23	— 23	—22
	Potsdam ...	— 3	— 3	— 1	1	4	7	11	14	14	11	6	— 1	— 7	—12
Ver. Intensity.	Tromsø	0	6	16	28	30	— 2	—26	—38	—35	— 6	40	86	130	180
	Abisko	10	10	25	40	35	22	10	10	20	40	80	140	200	233
	Sodankylä ..	12	17	20	25	42	52	48	32	8	— 8	— 12	30	95	95
	Lerwick	— 4	0	8	15	24	40	48	40	20	—10	— 45	— 86	—116	—138
	Lovø	0	4	17	23	37	44	52	50	40	20	0	— 18	— 40	— 60
	Rude Skov .	0	4	11	22	30	31	32	27	18	3	— 10	— 25	— 37	— 46
	Potsdam ...	— 3	— 4	3	— 2	1	5	8	12	14	11	6	0	— 8	— 13

5. THE CHARACTERISTICS OF THE PERTURBING VECTOR AT TROMSØ

In the previous chapters the characteristics of the *D*-field have been discussed, using the material from a net of recording stations, and we thus obtained a picture of the geographical distribution and the dynamical character of the *D*-field. In earth-magnetic investigations the point of view has often been *D*-field to use the material from a single station for discussing the characteristics of the *D*-field. This must be regarded as a method more than doubtful; the point of view should rather be from the known main features of the *D*-field to explain the characteristics of the perturbing vector at the recording station. An analysis of the mean perturbing vector at Tromsø in the horizontal plane and in the vertical plane, is given below.

In the year-books from Tromsø the monthly mean values of the perturbing vectors in the horizontal plane and in *Z* have been published since 1930. The mean diurnal variation of the perturbing vectors in the horizontal plane has been demonstrated in figures which in the literature has been named the „fish-bone" diagram—a mode of representation first used by Birkeland, and which we, below, call a Birkeland-diagram. The mean monthly Birkeland-diagrams in *H* during the whole period 1930—44 show a similar character from year to year. During years of maximum activity the vectors increase, but the directions are almost identical from maximum year to minimum year and also from summer to winter. For the perturbing vectors in vertical direction, *Z*, however, there is a variation from month to month which often may give the impression of being quite irregular.

From the characteristics of the *D*-field we know from the preceeding chapters, that there is a gradual displacement of the whole field towards lower latitudes with increasing earth-magnetic activity, an effect which will strongly influence and may even reverse the direction of the perturbing vector in *Z* at the individual recording

tories. The nine greatest storms in the period 1932—37 have been selected.

time

1	2	3	4	5	6	7	8	9	10	11	12	13
— 56	—100	—145	—157	—130	— 80	— 43	— 22	— 16	— 15	— 16	— 10	4
— 76	— 90	— 97	— 98	— 82	— 65	— 45	— 25	— 8	— 4	— 2	6	20
—120	—140	—140	— 85	— 50	— 34	— 23	— 10	0	8	12	8	0
— 33	— 31	— 25	— 17	— 10	— 4	— 1	— 2	— 3	— 2	0	1	1
— 27	— 16	— 10	— 7	— 6	— 5	— 3	— 3	— 3	— 4	— 3	— 2	2
— 22	— 16	— 12	— 9	— 6	— 3	— 1	0	0	3	5	8	10
— 20	— 12	— 10	— 9	— 8	— 6	— 5	— 4	— 3	0	2	3	4
—370	—420	—465	—460	—350	—190	—100	— 35	22	73	110	130	160
—408	—465	—478	—435	—255	—150	— 80	— 45	— 10	25	60	106	135
—470	—465	—410	—375	—250	— 80	— 50	— 30	0	30	75	110	115
—165	—160	—102	— 62	— 49	— 40	— 33	— 28	— 27	— 23	— 14	6	22
— 45	— 44	— 43	— 43	— 43	— 43	— 42	— 39	— 35	— 31	— 26	— 18	— 3
— 19	— 18	— 18	— 20	— 28	— 34	— 40	— 42	— 43	— 40	— 32	— 14	— 3
— 18	— 23	— 24	— 23	— 16	—12	— 7	— 3	0	2	5	7	10
220	236	200	104	30	— 12	— 20	— 14	0	10	8	10	30
243	200	105	— 60	— 80	— 30	— 25	5	25	40	44	38	15
20	— 50	—120	—160	—160	— 80	— 35	— 10	18	35	48	52	50
—160	—164	—150	—108	— 64	— 40	— 22	— 8	12	22	25	24	23
— 85	—103	—110	—100	— 78	— 50	— 25	— 9	2	16	25	33	40
— 53	— 63	— 60	— 43	— 27	— 18	— 10	— 3	3	12	19	25	32
— 18	— 22	— 24	— 22	— 17	— 12	— 7	— 3	— 1	2	7	10	10

station, whereas in H there is only a gradual variation in magnitude. We may therefore assume that the apparently irregular variations in the mean monthly values of $\triangle Z$ is due to the averaging of days with different magnitudes of storminess.

In order to investigate this point more closely, the material from Tromsø in the period 1930—44 was divided into nine ranges according to the magnitudes of storminess. In table 9 the daily sums of storminess (AS) for each of the nine ranges are given. Ten to twenty days within each range were selected and averaged. In fig. 19 is shown the mean vector diagrams in a horizontal and vertical plane for each of the nine ranges of disturbance. In the two vertical columns to the left the Birkeland-diagrams are drawn, and in the two columns to the right, the diurnal variation of the vectors is given in another mode of representation often used in literature.

From fig. 19 it is evident that the vector diagrams in the horizontal plane are similar for all ranges of disturbance. In the vertical direction, however, there is a gradual change with increasing earth-magnetic activity. It is evident that this is explained by a gradual displacement of the disturbing current system towards south with increasing earth-magnetic activity. Quantitatively, we may follow the displacement in the variation of the angles β_1 and β_2, defined in fig. 19. The angles α_2 and α_2 show only small variations with increasing ranges of disturbance. In table 9 the results from fig. 19 are summed up quantitatively.

Table 9.

Range	AS	α_1	α_2	β_1	β_2	d mean
1	0— 500	—	19°	39°N	39°N	130km N
2	500—1000	—	14	22	11	45
3	1000—1500	—	13	24	11	45
4	1500—2000	—	11	3 S	8 S	15 S
5	2000—2500	14	17	0	18	24
6	2500—3000	14	15	8	23	42
7	3000—3500	15	18	17	12	40
8	3500—4000	—	—	14	25	54
9	> 4000	14	18	4	18	(30)
	Mean	14	16			

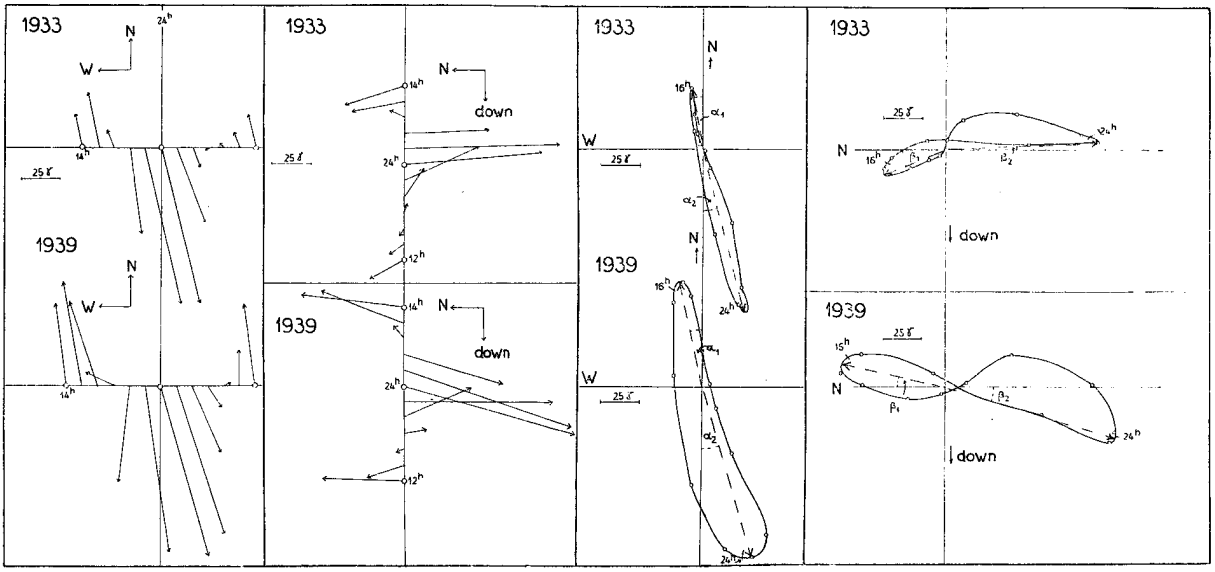

Fig. 20. Vector diagrams in horizontal and vertical planes for the minimum year 1933 and the maximum year 1939 at Tromsø.

In table 9 the mean distance d mean from Tromsø, north or south to the perturbing current system, has been calculated for the maximum phases at about 16^h and 24^h, assuming a height of the currents above the earth's surface, of 150 km.

The gradual changes of the vector diagrams with increasing storminess are of course also the cause of the different characters of the vector diagrams from summer to winter seasons and from years of minimum solar activity to years of maximum solar activity. In order to demonstrate this, the vector diagrams for Tromsø for the minimum year 1933 and the maximum year 1939 are drawn up in fig. 20, and table 10 gives the mean position of the current system at about 16^h and 24^h.

Table 10.

	α_1	α_2	β_1	β_2	d mean
1933.....	11°	14°	21° N	3° N	32 km N
1939.....	13°	16°	12° S	16° S	38 km S

In a year of minimum solar activity the current system at the hours of maximum, 16^h and 24^h, lies about 30 km *north* of Tromsø, in a maximum year, the current system lies about 40 km *south* of Tromsø at the corresponding hours.

6. THE PROPERTIES OF THE IMPETUS-VECTOR

In a number of cases great magnetic storms start with a sudden commencement. In the records, the sudden commencement (*SC*) or *impetus* is marked out as a sudden and sharp deflection which appears in all the three components. The outswing of the *SC*-deflection attains its maximum value in the course of about one minute, then the deflection is reversed and a similar deflection appears in the opposite direction. These two phases of a *SC* are only visible on records of good qualities. The first deflection, which we shall call the primary impulse (P), is usually much less developed than the second deflection, the secondary impulse (S), and may easily be overlooked, especially on records from lower latitudes. The outstanding character of the impetus makes it worth while to investigate the properties of the perturbing vector at the moment when the impetus deflection has its maximum values in the P- and S-impulses. For these investigations the original records from Tromsø, Abisko, Lovø and Niemegk were inspected, and 17 cases of well developed *SC* were measured out. In fig. 21 is shown one example of a *SC* recorded on three observatories.

In table 11 are given the results of the measurements of the records, and in table 12

the mean values at the four observatories are summed up.

Here $\triangle D$, $\triangle H$ and $\triangle Z$ are the maximum deflections. P_H is the perturbing vector in the horizontal plane. α is the angle in the horizontal plane between the N—S direction and P_H. β is the angle between the Z-direction and the perturbing vector. Fig. 22 shows the position of the perturbing vector in a horizontal and vertical plane for the 17 cases for Niemegk, and fig. 23 the position of the mean vectors in a horizontal and vertical plane.

There is a considerable decrease in the magnitude of the P-impulse from Tromsø to Niemegk, whereas the magnitude of the S-impulse maintains its order of magnitude. The P- and S-vectors are opposite-directed, with the horizontal components lying approximately in the geomagnetic meridian. In the vertical plane, the perturbing vectors show approximately the same elevation above the earth's surface for all four observatories, although the inclination is decreasing with about 10° from Tromsø to Niemegk. Below in fig. 23 the position of the perturbing vector of the S-impulse at Watheroo from dates published by McNish has been drawn up for comparison. The mean vector for Watheroo has been calculated from 155 single cases. There is an astonishingly close similarity between the position of the mean vectors when going from the northern to the southern hemisphere. In the horizontal plane, P_H for Watheroo lies in the geomagnetic meridian, and in the vertical plane the angle of elevation for the perturbing vector is of about the same value as on the northern hemisphere. It must be borne in mind, however, that the material from high northern latitudes and from Australia is not identical, and an investigation of simultaneous cases is still lacking.

Concerning the time interval $\triangle t$ between the maximum peak in the P- and S-impulse, a number of measurements has been made on a number of well developed cases. Values of $\triangle t$ of 3.2, 3.2, 2.5, 3.0, 3.2, 3.8, 3.5 and 3.8 minutes, with a mean value of $\triangle t = 3.2$ minutes were found. We here assume that the maximum value of the deflection is attained exactly at the same time in all three components. With the limited accuracy of the normal records of a speed of one hour per twenty cm it is not possible to fix the timing of

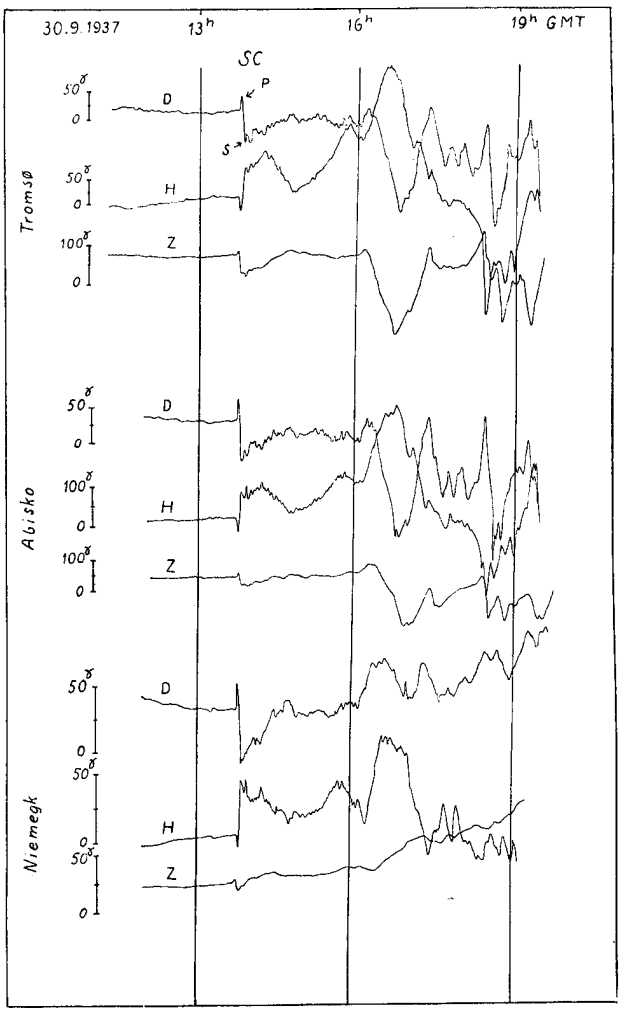

Fig. 21. Records from Tromsø, Abisko and Niemegk showing the character of a sudden commencement (SC) with well developed primary (P) and secondary (S) impulses.

a deflection with greater accuracy than say half a minute. For a still closer examination, for instance of a phase difference between the impulses in the three components, rapid registrations must be available.

We have hitherto assumed that the perturbing vectors of the P- and S-impulses during the whole process of the SC lie uniformly in the directions of the mean vectors shown in figs. 22 and 23. If there is an even small phase difference between the deflections in the three components there will, however, be a rotation of the perturbing vector which may alter the picture of the process here given to some extent.

As previously mentioned, there are still doubts about the natur of the disturbing currents

Table 11.

No.	Date	GMT	Tromsø						Abisko					
			P-impulse			*S*-impulse			*P*-impulse			*S*-impulse		
			ΔD	ΔH	ΔZ	ΔD	ΔH	ΔZ	ΔD	ΔH	ΔZ	ΔD	ΔH	ΔZ
			γ	γ	γ	γ	γ	γ	γ	γ	γ	γ	γ	
1	30. 4. 1933	16h29m	— 10.8	— 56.0	5.2	27.6	65.0	(47.0)	— 9.6	— 39.9	8.0	26.0	84.0	
2	27. 1. 1935	14 51		— 38.0		32.6	26.0					37.0	37.1	— 11.0
3	30. 3. »	12 12	— 21.3	— 45.5	8.4	34.6	46.0	— 37.4	— 19.2	— 38.5	6.1	34.0	57.4	— 15.0
4	7. 7. »	21 8	— 14.4	— (5.0	3.4	40.0	(9.0)	— 23.1						
5	2. 10. »	17 22							— 2.4	— 7.0	8.8	13.3	57.6	
6	2. 2. 1937	23 5	— 1.0		1.4	26.0	16.5	— 39.4	— 2.4		3.3	26.1	40.8	— 36.0
7	18. 2. »	19 6												
8	25. 2. »	11 44	— 15.0	— 21.5	6.2	20.0	32.0	— 15.0	— 17.8	— 23.8	4.4	16.6	35.0	— 17.6
9	26. 3. »	20 57	— 5.0			19.5	16.0	— 17.7	— 3.7		1.8	19.2	22.4	— 23.0
10	21. 5. »	15 59	— 4.8	— 6.0		20.0	55.0	— 42.0	— 5.2	— 5.6	1.1	20.7	72.1	— 22.0
11	22. 8. »	3 6	— 27.6		2.7	38.4	34.5	— 17.7						
12	30. 9. »	13 45	— 35.0	— 25.0	11.8	57.6	40.0	— 42.0	— 30.3	— 35.7	8.0	59.2	68.0	— 23.0
13	27. 4. 1939	21 1												
14	27. 5. »	20 54							— 4.3	— 2.1	1.8	29.6	15.4	— 18.0
15	20. 7. »	22 3												
16	2. 10. »	21 42												
17	11. 10. »	19 44							— 3.7		1.8	23.3	14.7	— 23.0
		Mean:	— 15.0	— 28.1	5.6	31.6	34.0	— 31.2	— 9.9	— 21.8	4.5	27.7	45.9	— 21.0

producing the earth-magnetic storms, whether these are to be regarded as free corpuscular currents in Birkeland's sense, or, whether they are flowing as convection currents in the upper atmosphere. Concerning the primary cause of the storms, however, there is general agreement that this is caused by the approach of swarms of corpuscles reaching the earth. The *SC* represents the first terrestrial effect of these swarms of corpuscles and is therefore of special interest.

The amplitude of a common polar storm decreases very rapidly with increasing distance from the auroral zone. During the maximum phase at midnight, for instance, the mean deflection in H in Lovø is only about 1/10 of the deflection in Tromsø, and in Niemegk the deflection is still less. The deflections in the *SC*, and mainly the *S*-impulse, however, are roughly independent of the distance from the auroral zone. If we assume that the deflection of the *SC* is caused by any free corpuscular current system, this current system must lie at a distance from the earth far greater than the dimensions on the earth's surface.

Qualitatively the directions of the perturbing vectors of the *P*- and *S*-impulses may be explained by the effect of a ring-current forming a ring or cylindrical sheet symmetrical to the earth's equator and with a radius far greater than that of the earth. In fig. 24 the positions of the perturbing vectors in a meridian plane have been

Table 12.

	P-impulse				*S*-impulse									
	ΔD	ΔH	ΔZ	ΔP_H	ΔD	ΔH	ΔZ	P_H	α_P	α_S	β_P	β_S	ψ'	90—I
	γ	γ	γ	γ	γ	γ	γ	γ	°	°	°	°	°	°
Tromsø	—15.0	—28.1	5.6	31.8	31.6	34.0	—31.2	46.4	28	43	10	34	30.8	12.4
Abisko	— 9.9	—21.8	4.5	24.0	27.7	45.9	—21.0	53.6	24	31	11	21	29.3	13.7
Lovø	— 6.6	— 5.8	(4.1)	8.8	19.6	30.6	— 8.0	35.0	49	33	(25)	13	22.1	18.5
Niemegk	— 5.6	— 4.1	1.4	6.9	17.8	37.3	— 8.5	41.3	54	26	12	14	18.8	23.2

Lovø						Niemegk					
P-impulse			*S*-impulse			*P*-impulse			*S*-impulse		
$\triangle D$	$\triangle H$	$\triangle Z$	$\triangle D$	$\triangle H$	$\triangle Z$	$\triangle D$	$\triangle H$	$\triangle Z$	$\triangle D$	$\triangle H$	$\triangle Z$
γ	γ	γ	γ	γ	γ	γ	γ	γ	γ	γ	γ
						— 3.9	— 14.6	3.9	13.2	39.6	— 13.8
							— 2.0	1.8	19.5	34.5	— 8.3
						— 9.9	— 6.5	1.5	21.3	31.5	— 7.0
						— 5.4	— 2.2	0.7	20.5	36.5	— 8.3
— 0.5	— 4.8		8.0	21.6	— 3.3		— 3.9	0.7	7.6	20.7	— 5.1
— 1.5	— 1.6		20.3	40.0	— 8.9	— 1.2	— 1.2		21.0	46.2	— 11.5
						— 1.2	— 0.6		8.0	34.5	— 8.9
— 9.9	— 13.6	2.2	17.5	21.6	— 7.8	— 9.4	— 5.1	0.9	17.5	26.0	— 5.5
— 3.1	— 0.8		13.5	30.6	— 8.9	— 2.1	— 1.6		11.3	38.6	— 8.8
— 3.6	— 11.2	2.2	12.5	44.0	— 11.2	— 3.1	— 7.3	1.4	12.8	36.5	— 6.9
— 14.4	— 0.8	2.2	26.1	24.0	— 8.9	— 11.3	— 1.0		25.2	18.3	— 4.8
— 18.0	— 14.4	10.0	40.6	44.0	— 17.3	— 18.8	— 7.7	1.8	29.2	40.6	— 6.2
— 2.7			19.2	24.0	— 2.2	— 1.9			16.3	36.5	— 7.4
— 2.7	— 0.8		22.3	22.4	— 3.4	— 1.9		0.5	21.7	34.1	— 6.4
— 11.1	— 8.0		18.0	32.0	— 10.0				19.2	54.8	— 12.4
						— 7.2	— 2.0		23.3	66.0	— 15.0
— 3.6	— 1.6		18.0	32.0	— 5.6	— 1.6	— 1.6	0.5	15.5	39.0	— 8.3
— 6.6	— 5.8	(4.1)	19.6	30.6	— 8.0	— 5.6	— 4.1	1.4	17.8	37.3	— 8.5

drawn up for the five recording stations. For a ring-current lying in the equator, the perturbing vector should of course be directed along the N—S direction. But we must assume that the induced earth currents to some extent may modify the initial perturbing vector.

This point of view for explaining the properties of the *SC*-vectors may be said to fit well in with the corpuscular theory of the earth-magnetic storms. The initial phase of the storms during which a *SC* is developed, may be the formation of a ring current. During the weaker first phase, the *P*-impulse, of the *SC*, the current flows in a direction opposite to that which the current has during the stronger *S*-impulse. (We may regard it as probable that for Watheroo, McNish has neglected the appearance of the weaker *P*-impulse. The absence of the *P*-vector for Watheroo on the figures is therefore no proof of its non-existence). The existence of two different impulses in the *SC* may be explained if we assume that the swarm of corpuscles is of different signs, a „head" of one sign followed by a „tail" of an opposite sign arriving at about 3 minutes later.

In the discussions of the corpuscular theories of the aurorae and magnetic storms by different authors (Vegard, Chapman and Alfvén) one generally now regards the swarm of corpuscles approaching the earth as consisting of positive and negative particles. Chapman has especially discussed this problem quantitatively, and in his theory of magnetic storms he regards the swarm of particles to be of different signs and mainly separated in a „head" and a „tail" of different particles. The formation of a ring-current of different signs should therefore alternate in succession of about 3 minutes, corresponding to the time difference between the *P*- and *S*-impulses.

A time difference in arrival of about 3 minutes of the „head" and the „tail" of a swarm of particles, presupposes that the velocity of the particles is low. This brings us to the most critical question in the corpuscular theory of the aurorae and the earth-magnetic storms, namely, the nature and velocity of the particles. From auroral studies, especially of the nature of the spectrum and the penetration depths of the aurorae, one is apt to assume swift particles, presumably of the cathode-ray type. For the corpuscles producing the earth-magnetic storms,

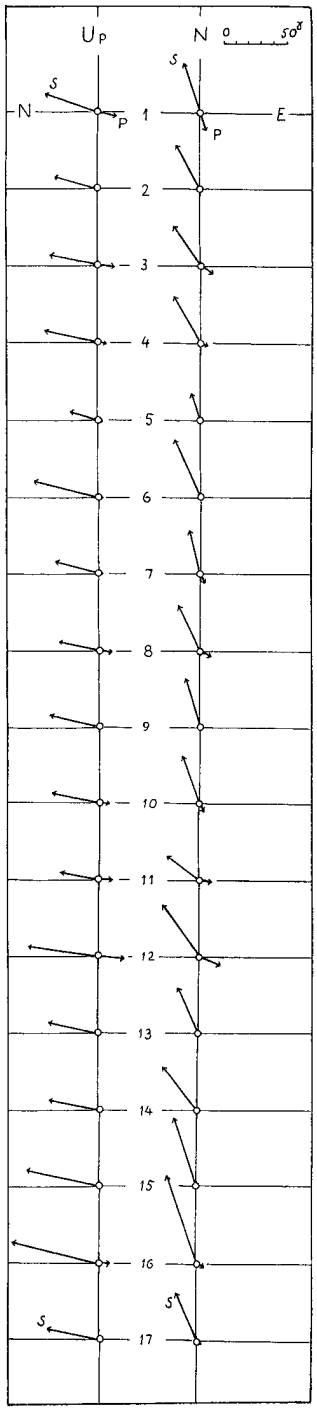

Fig. 22. Position of single cases of the impetus vectors in a horizontal and vertical plane for Niemegk. *P* and *S* denote the primary and secondary impulses.

however, there are certain indications that the velocity of the particles is low. We may in this connection mention that there is a time-difference of somewhat more than one day between the passage at the central meridian on the sun of a great sunspot and the start of the following earth-magnetic storm. More convincing than these statistical results, however, are the number of cases which Hale[1] has observed and described. From his observations of very great solar eruptions, by means of the spectro-helioscope, he states that the following great earth-magnetic storm started on an average about 26 hours later. This leads to a velocity of the particles of only 1.6×10^8 cm/sec. A possible solution between these two opposing alternatives of swift and slow particles, is the assumption that the aurorae and the earth-magnetic storms are really produced by different types of radiation, one swift for aurorae and another type of slow particles for earth-magnetic storms. As we shall see in the following section, there is, however, a close parallelism between the auroral luminosity and the magnitude of the earth-magnetic deflection when the aurorae are overhead. This makes the assumption of two different and separate groups of particles producing aurorae and earth-magnetic storms which arrive at different times, highly improbable.

[1] Referred by Grotrian in Naturwiss. *19*, 193 (1931) and *21*, 55 (1932).

Section II.

1. REGISTRATION OF THE AURORAL LUMINOSITY DURING EARTH-MAGNETIC STORMS

The problem of getting a complete and objective record of the auroral activity has always encountered great difficulties in auroral research. A complete record should give information of

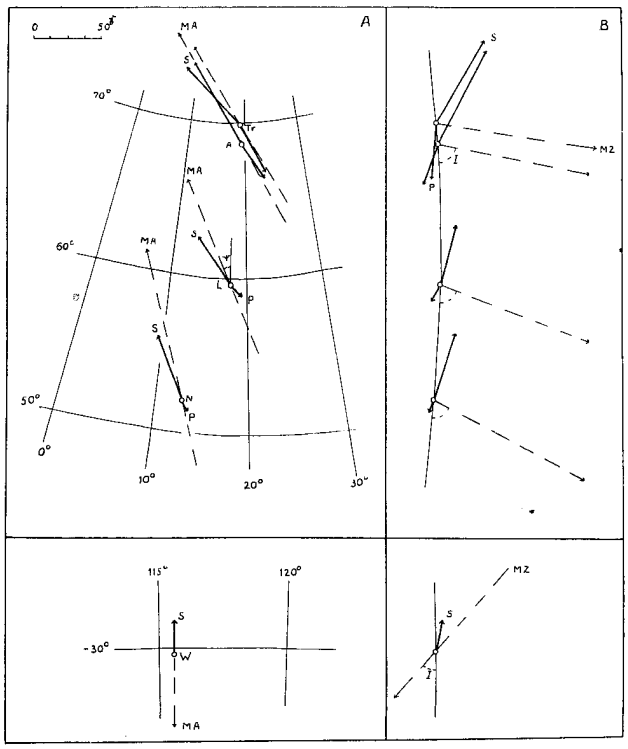

Fig. 23. Position of the mean values of the impetus vectors at the four observatories in a horizontal (*A*) and vertical (*B*) plane. *MA* denotes the direction to the magnetic axis' point and *MZ* to magnetic zenith. Below is the mean vector of the *S*-impulse for Watheroo (Australia) indicated (from dates given by McNish[1]).

[1] See Terrestrial Magnetism and Electricity edited by Fleming, p. 378.

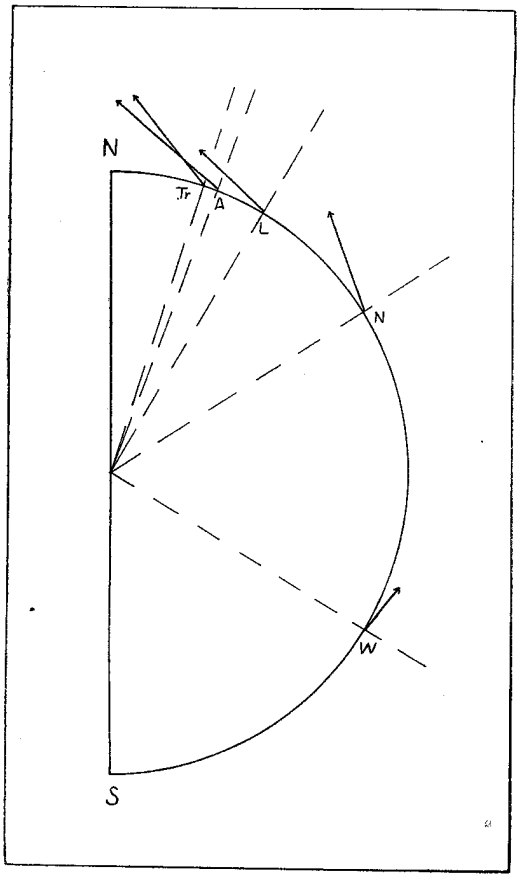

Fig. 24. Position of the perturbing vectors in a meridian plane of the S-impulses.

the luminosity and extension of the aurorae and the type and position on the sky. Up to now, it has therefore often been considered that a careful written auroral log would give the most complete information.

Different methods of objective registrations have been tried. Photo-cells have been used by

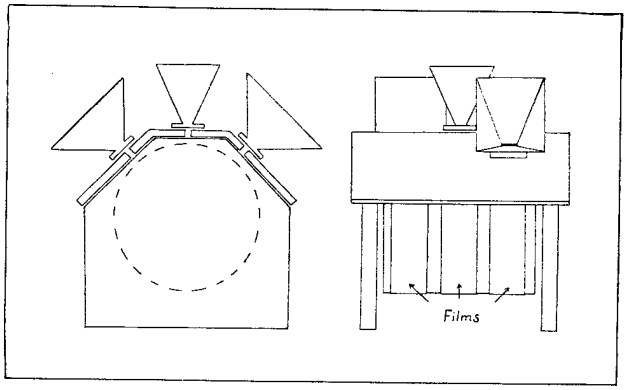

Fig. 25. Auroral recorder, schematically. The integrated luminosity is recorded on three strips of films, the northern sky, zenith and the southern sky separately.

several observers and photographic photometric measurements have been tried by others. For laboratory use a photo-electric cell supplied with amplifier and a recording instrument is easy to operate, but during severe weather conditions in winter time, delicate instruments as photo-cells and amplifiers are less suitable for continuous registrations. During the winter 1944—45, a photographic photometric registration of the auroral luminosity was developed which was reliable to operate and seemed to give reliable results, and which it is intended should be in continuous use at the observatory. Fig. 25 shows the construction of the auroral recorder.

The integrated luminosity is recorded on three strips of films, the northern sky, zenith and the southern sky separately. By special lamps (not shown in the figure) the films were supplied with time marks. The whole recorder was mounted in a light tight box supplied with automatic shutters which closed before sunrise. Some of the records are shown on Plate I.

For statistical studies, the material from

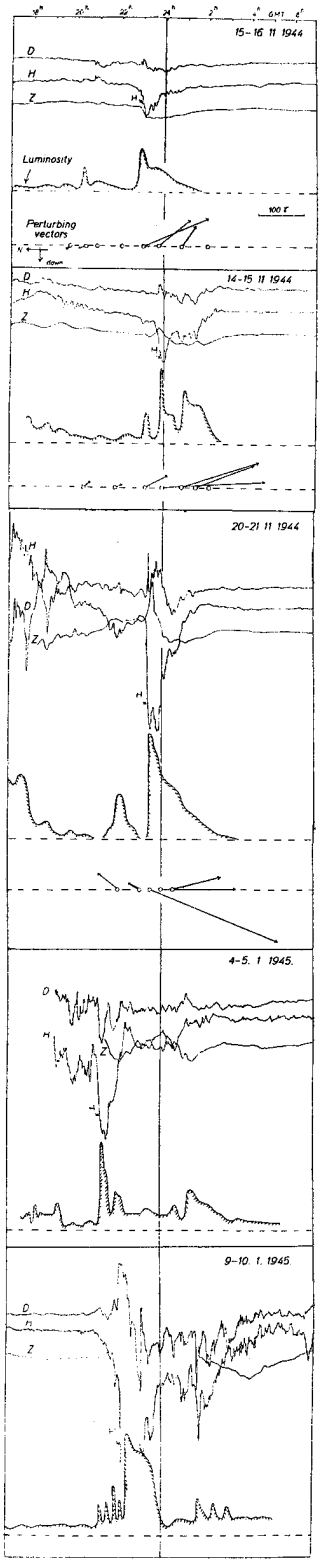

Fig. 26. Variations of the auroral luminosity during days of increasing earth-magnetic activities.

the autumn 1944 is not sufficient, but a number of records demonstrate the close connection between the auroral luminosity and the degree of earth-magnetic storminess. In fig. 26 the records from five days with increasing earth-magnetic activities have been drawn up. In each case there is a close connection between the amplitude in H and the variation in the integrated auroral luminosity. On the three first days, the positions of the perturbing vectors lying in a vertical plane in N—S direction, have been drawn up. On the first day, the perturbing vectors indicate that the perturbing current system was lying considerably north of Tromsø. The second day the perturbing current system was lying closely north of Tromsø, and, on the third day, the perturbing current system during the maximum deflection in H, was lying slightly south of Tromsø. The auroral records indicate a parallel increase in the total integrated luminosity. A full discussion of the variation in the auroral luminosities north and south of zenith during earth-magnetic storms can first be given only when a more extensive material has been collected.

It would be of special interest to follow the variations in the auroral luminosities during the hours when the storminess in H changes from positive to negative values. According to the figures 6—9 there is here a discontinuity in the „auroral zone", and it would be of great interest to see if the same discontinuity appears in the auroral luminosity curves.

SUMMARY

The mean field of disturbance, the D-field, during polar earth-magnetic storms has been studied by means of records from stations between Spitzbergen and Niemegk. The mean diurnal variation of the field across a geomagnetic meridian at about $\Lambda = 120°$ has been demonstrated on maps in all three components and for four different degrees of storminess.

The position of the current system, or „auroral zone", has been determined for different degrees of storminess. The dimensions of the perturbing current system, height and current intensity, have been calculated, and it is shown that an assumed internal part of the perturbing vector due to earth currents of 0.4 is inconsistent with the observations. The observations indicate that the effect of the earth-currents seems not to exceed 0.1 of the perturbing force recorded. The characteristics of the mean perturbing vectors at Tromsø are discussed, using the model currents from the analysis of the D-field.

A study of simultaneous appearing SC in the records from four observatories is given. It is shown that the main characteristics of the impetus-vector can be roughly explained by the assumption of a ring-current outside the earth lying on the equator.

A method of recording the auroral luminosity is described, and the connection between auroral luminosity and earth-magnetic perturbations is discussed on a number of records.

Printed November 5th, 1946.
GRØNDAHL & SØNS BOKTRYKKERI

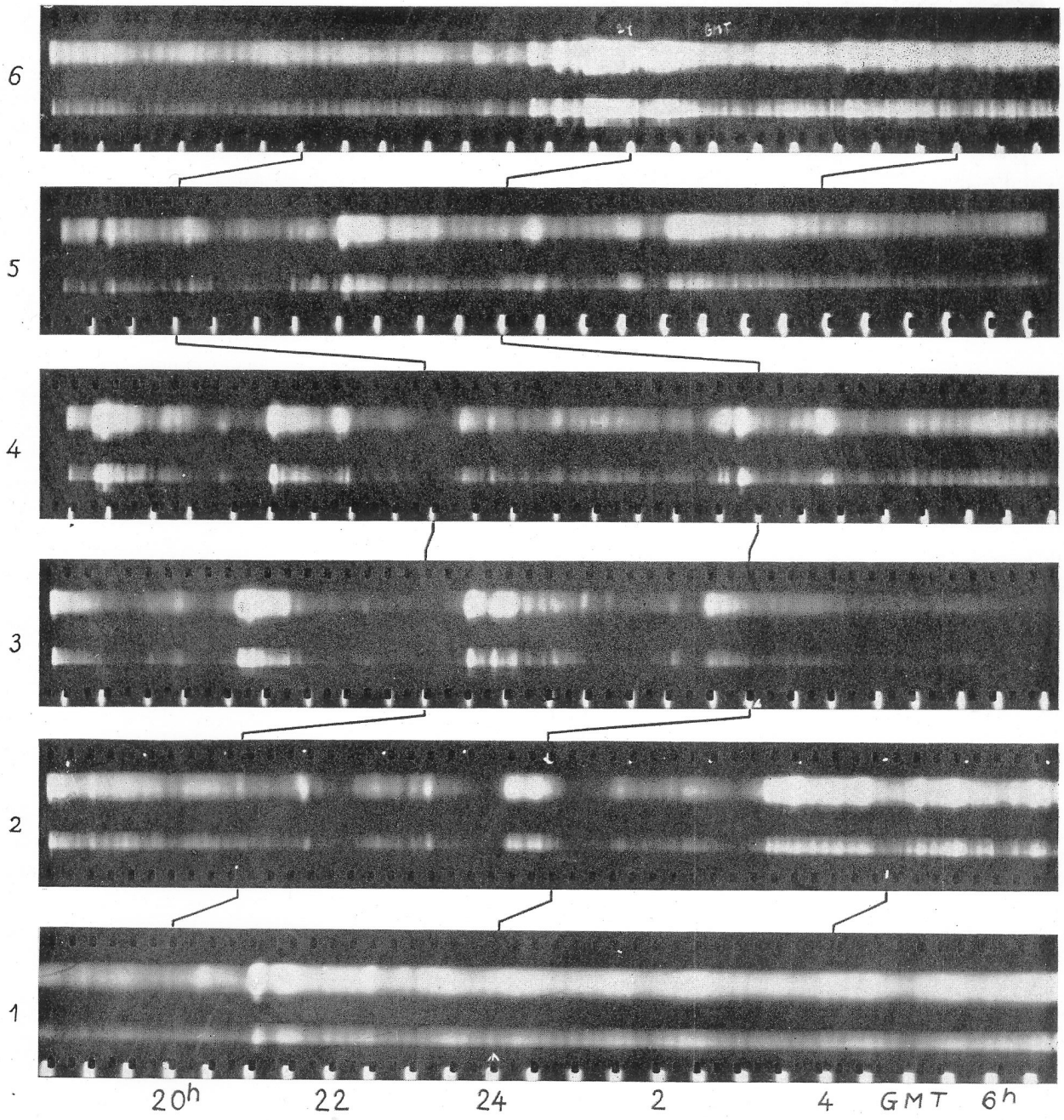

Explanation to Plate I.

Records of the integrated luminosity of the aurorae during the night. Light marks each half hour are shown below on each record.

No. 1 — 6– 7. 12. 1944,
2 — 13–14. 12. 1944,
3 — 16–17. 12. 1944,
4 — 17–18. 12. 1944,
5 — 4– 5. 1. 1945,
6 — 9–10. 1. 1945.